International Journal of Chemistry; Vol. 11, No. 2; 2019
ISSN 1916-9698 E-ISSN 1916-9701
Published by Canadian Center of Science and Education

Derivation of a pH Dependent Solid-Liquid Interfacial Tension and Theoretical Interpretation of the Physicochemistry of Dewetting in the CO_2-Brine-Silica System

Mumuni Amadu[1], Adango Miadonye[2]

[1]Graphite Innovation Technology Inc. and part time Faculty, Process Engineering and Applied Science, Dalhousie University, Canada

[2]Department of Chemistry, Cape Breton University, Canada

Correspondence: Mumuni Amadu, Graphite Innovation Technology Inc. and part time Faculty, Process Engineering and Applied Science, Dalhousie University, Canada. E-mail: mm846771@dal.ca, mumuniamadu@hotmail.com

Received: August 1, 2019 Accepted: August 25, 2019 Online Published: September 4, 2019

doi:10.5539/ijc.v11n2p127 URL: https://doi.org/10.5539/ijc.v11n2p127

Abstract

The solid-liquid interfacial tension is a fundamental parameter in areas of wettability pertaining to adhesive bonds and petroleum engineering practice. In wettability issues related to surface functionalized polymeric materials design to achieve specific adhesive properties, the solid-liquid interfacial tension can be pH dependent due to amphoteric behavior. In this paper, we have used the theory of pH dependent surface charging and the 2-pk model as well as the site binding model of the electric double layer theory to derive a pH dependent solid-liquid interfacial tension equation.

Following the fundamental relationship between solid-liquid interfacial tension and contact angle in light of Young's equation, we have extended the theoretical basis of the derivation. Consequently, we have also derived a pH dependent cosine of the thermodynamic contact angle. Both equations give satisfactory explanations for observed experimental data available in the literature.

Keywords: solid-liquid interfacial tension, surface charge, wettability, point of zero charge pH, physiochemistry

1. Introduction

In the context of wettability, three fundamental interfacial parameters are critical to defining the thermodynamic contact angle. They are solid-gas interfacial tension, fluid-fluid interfacial tension and solid-liquid interfacial tension (Fernandez-Toledano *et al*., 2017). All interfacial tensions are the direct results of intermolecular interactions at interfaces, which involve dispersion (Fowkes, 1964) and nondispersion contributions (Carre, 2007). Regarding Young's equation, changes in interfacial tensions or any of the interfacial tensions will result in contact angle change (Lubetkin & Akhtar, 1996). Considering the solid-liquid interfacial tension, changes can be brought about in two distinct ways. One is the change in the chemistry of the fluid, which can be brought about by changes in aqueous species concentration or ionization of acidic or basic components of fluids following pH changes as encountered in the case of crude oil in petroleum reservoirs (Hutin *et al.,* 2016)**.** The other mechanism involves change in the solid surface free energy due to protonation and deprotonation reactions of surface functional groups following pH changes (Lowe *et al*., 2015)**.**

In the literature, Vitoz *et al* (1998) have given a theoretical plot of solid-liquid interfacial tension versus pH**.** Barrancor Jr *et al*., (1997)**,** have also given a plot of solid-liquid interfacial tension versus pH for varying concentrations of aqueous solution. Also, experimental data have been fitted to contact angle versus pH data (Trevino, *et al*., 2011; McCafferty & Wightman, 1997;Orumwense, 1998;Orumwense, 1998;Orumense, 2001). On the other hand, the pH dependence of solid-liquid interfacial has been explained in the work of Chatelier *et al*., (1995); while the pH dependence of polar contributions to solid-liquid interfacial tension has also been explicitly given in the work of Glover *et al*, (1994)**.**

Following the effect of surface excess adsorption on solid-liquid interfacial tension, Gibbs equation relates change in solid-liquid interfacial tension to the chemical potential of species and the surface excess adsorption parameter (*Vitoz et al*., 1998). Assuming a Nearnstian surface, there is a fundamental relationship between change in surface potential of solid surface and the pH of aqueous solution in contact with it. What is more, the thermodynamics of the solid-liquid interface (Chattoraj & Birdi, 1984), provides additional literature for a thorough understanding of the physics of the solid-liquid interface. Therefore, we think that given the theoretical bases of all the above mentioned physiochemical processes

directly linked to wettability and or contact angle, a rigorous approach can be used to mathematically describe the solid-liquid interfacial tension dependence on aqueous solution pH, which will serve as a tool for theoretically understanding existing solid-liquid interfacial tension versus pH trends in the literature. Thus, given the direct relationship between solid-liquid interfacial tension and contact angle in light of Young's equation, trends in contact angle variation with pH of aqueous solution will be amenable to explanation based on the outcome of our mathematical model. We will pursue this objective at the appropriate section.

2. Literature Review

2.1 Physiochemistry of Wetting

Wettability is the preference of a fluid phase for a solid surface where two or more fluids exist in addition to a solid surface (Schön, 2015), and the physicochemistry of wetting involves the physical and chemical processes that occur together to alter wettability or impart a dynamic character to it (Caroline-Michaliski & Saramago, 2000). Such processes span two notable areas of scientific research and advancement; they include intermolecular forces contribution to interfacial free energy/interfacial tension, which integrates additive and nonadoptive terms (Oss *et al*., 1988) and processes directly related to surface adsorption, which affect the nonadditive terms of interfacial free energy/tension.

The existence of forces between molecules and atoms was first put forward by van der Waals (Buckingham *et al.*, 1988)**.** At the interface between two phases, intermolecular forces will be manifest. These forces can be electrodynamic in origin, consisting of randomly oriented dipole interactions, random orienting dipole-induced dipole interactions called Debye interaction and fluctuating dipole-induced dipole or dispersion interaction originally described by London (Oss, 2006), and generally considered to be universal. The first two were later found to be similar to the third one, following which the three electrodynamic forces became jointly known as van der Waals forces. Apart from intermolecular forces of electrodynamic nature, other intermoleculer forecs inreractions occur that are electrostatic or polar in origin (Bradely, 2005).

Interfacial free energy is the work done to create a unit interface area between phases and it is numerically equal to the interfacial tension (force/unit length) for the case of liquids (Orowan, 1970). Interfacial tension is a direct outcome of Lishfizt van Der Waals forces. Accordingly, the interfacial free energy or interfacial tension can be quantified in terms of intermolecular forces, given for phase 1 and phase 2 as (Oss, 2006):

$$\gamma_{12}^{LW} = \gamma_1^{LW} + \gamma_2^{LW} - 2\sqrt{\gamma_1^{LW}\gamma_2^{LW}} \tag{1}$$

in which $\gamma_{12}^{LW}$is the interfacial tension between phase 1 and phase 2, $\gamma_1^{LW}$is the surface tension of phase 1 and, γ_2^{LW} is the surface tension of phase 2, all due to Lishfizt van der Waals forces (LW).

Apart from electrodynamic van der Waal forces contribution to interfacial tension, there are acid-base interactions of polar nature as opposed to nonpolar dispersion forces described by Lewis (Oss, 1993). These polar contributions are known as electron acceptor or electron donor components (Bellon-Fontaine, 1996). Compared to Lishfizt van der Waals forces, the contribution due to acid-base interactions is stronger (Oss, 1993). In the context of wetting, the orginal interplay among these polar and nonpolar intermolecular forces at the three-phase contact line defines the ambient or staitc wettabilty state of a system (Jiang, *et a*l., 2016), while their evolution in response to changes in physiochenical conditions, such as system temperature, pressure, aqueous and non aqueous phase components concentrations and pH causes wettability change (Joud *et al*., 3013)**.** The case of pH change is directly linked to electrostitic charge and potential similar to the case of electric induced dynamic wetting in the field of electrowetting (Schneemilch *et al*., 2000).

Invoking the energy additivity theory of Fowkes (Oss, 1993), in the context of wetting physicochemistry, the interfacial tension is the sum of van der Waals electrodynamic and acid base contributions. This gives for phase 1 and phase 2 (Oss, 2006):

$$\gamma_{12} = \left(\gamma_1^{LW} + \gamma_2^{LW}\right)^2 + 2\left(\sqrt{\gamma_1^+\gamma_1^-} + \sqrt{\gamma_2^+\gamma_2^-} - \sqrt{\gamma_1^+\gamma_2^+} - \sqrt{\gamma_1^-\gamma_2^+}\right) \tag{2}$$

In which γ_1^- is the electron donor contribution to phase 1 surface tension , γ_1^+ is the electron acceptor contribution to phase 1 surface tension, γ_2^- is the electron donor contribution to phase 2 surface interfacial and γ_2^+ is electron acceptor contribution to phase 2 surface.

Physicochemical processes related to adsorption induced changes of solid-liquid interfacial tension have been well descibed in the literature (Ward & Wu, 2007; Ratajczak & Drzymala, 2012; Chattoraj & Birdi, 1984; Puah, *et al*., 20100)**.** In light of polar contributions to interfacial tesnion given by Eq. (2), adsorption of negatively and positively charged species in solution onto positively and negatively charged sites respectively on solids, which are the polar contributions

leads to solid-liquid interfacial tension changes. Since intermolecular interactions are responsible for interaction potentials, the total change in interaction energy for a system consisting of carbon dioxide-water-solid, where water and carbon dioxide interact through a solid phase can be equated to other interfacial components as (Oss, 2006)

$$\Delta G_{wrCO_2}^{TOT} = \gamma_{12}^{LW} - \gamma_{13}^{LW} - \gamma_{23}^{LW} + 2\left[\begin{array}{l}\left(\gamma_3^1\right)^{\frac{1}{2}}\left\{\left(\gamma_3^+\right)^{\frac{1}{2}} + \left(\gamma_2^-\right)^{\frac{1}{2}} - \left(\gamma_3^-\right)^{\frac{1}{2}}\right\} + \left(\gamma_3^1\right)\left\{\left(\gamma_1^+\right)^{\frac{1}{2}} + \left(\gamma_2^+\right)^{\frac{1}{2}} + \left(\gamma_3^+\right)^{\frac{1}{2}}\right\} - \\ \\ \left(\gamma_1^+\gamma_2^-\right)^{\frac{1}{2}} - \left(\gamma_1^-\gamma_2^+\right)^{\frac{1}{2}}\end{array}\right] \quad (3)$$

Subscript *r* refers to phase 3, 1 refers to water and 2 refers to CO_2

In this equation, γ_{13}^{LW} is the dispersion forces contribution to phase 1 and phase 3 interfacial tension, γ_{23}^{LW} is the dispersion force contribution to interfacial tension between phase 2 and phase 3, γ_3^+ is the electron acceptor contribution to phase 3 surface tension and γ_3^- is the electron donor contribution to phase 3 surface tension.

To quantify the effect of polar and nonpolar contributions on the wettability state of a system, the contact angle, which is directly linked to wettability and represents a universal parameter for describing the degree of wetting of a given surface by a fluid (Kozbial *et al*., 2017) has been linked to the total components of interfacial tension as (Oss, 2006):

$$\left(1+\cos\theta\right)\gamma_{CO_2-br} = \gamma_{12}^{LW} - \gamma_{13}^{LW} - \gamma_{23}^{LW} + 2\left[\begin{array}{l}\left(\gamma_3^1\right)^{\frac{1}{2}}\left\{\left(\gamma_3^+\right)^{\frac{1}{2}} + \left(\gamma_2^-\right)^{\frac{1}{2}} - \left(\gamma_3^-\right)^{\frac{1}{2}}\right\} + \left(\gamma_3^1\right)\left\{\left(\gamma_1^+\right)^{\frac{1}{2}} + \left(\gamma_2^+\right)^{\frac{1}{2}} + \left(\gamma_3^+\right)^{\frac{1}{2}}\right\} - \\ \\ \left(\gamma_1^+\gamma_2^-\right)^{\frac{1}{2}} - \left(\gamma_1^-\gamma_2^+\right)^{\frac{1}{2}}\end{array}\right] \quad (4)$$

In equation (4), θ is the thermodynamic contact angle.

In the following section, we will review the origin of the polar contributions to solid-liquid interfacial tension due to physicochemical processes, such as hydration and hydroxylation of solid surfaces, to reflect our principal objective.

2.2 Origin of Surface Functional Groups at the Solid-Liquid Interface

Surface functional groups play vital roles regarding physicochemical processes occurring on the surface of solids and they are directly responsible for pH induced wetting and dewetting at interfaces related to solid-liquid interfacial tension evolution. A surface functional group is defined as a chemically reactive molecular unit bound into the structure of a solid at its periphery, where the reactive components of the unit can be bathed by a fluid. These functional groups can be organic, such as carboxyl, carbonyl, phenolic or inorganic such as silanols (Arima & Iwata, 2007). In the context of the present paper, the major inorganic surface functional groups of interest are those associated with the plane of oxygen atoms bound to the silica tetrahedral layer of a tectosilicate or a phyllosilicate (Deer *et al*., 1962). Under normal room conditions (0%-30%) humidity, the surface of a solid has 3 molecular layers of water (Asay & Kim, 2005). Naturally, the surface of a solid, such as silica that is unhydrated will have metal ions that are Lewis acids, having reduced coordination numbers. The oxide anions will act as Lewis bases. The surface metal ions will coordinate to water molecules forming a Lewis acid site. A dissociative chemisorption reaction of water molecules on the surface of the solid leads to hydroxylated surface with surface OH groups (Tamura, *et al*., 2001). Figure 1 gives an example of hydration and hydroxylation reactions leading to the formation of surface functional groups on a metal oxide.

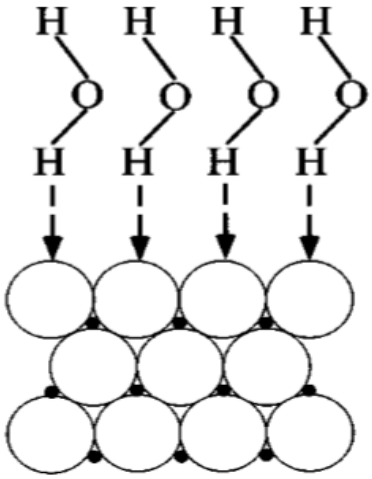

Figure 1. Hydration and Hydroxylation of metal oxide surface with the formation of acid base hydroxyl groups

The role of surface functional groups regarding the physicochemistry of wetting will be explained in the following sections.

2.3 Mechanism of Surface Charging

Surface charging is simply the process of charge development on a surface, through any of four basic mechanisms. The mechanisms involve adsorption reactions of ions on the surface, lattice substitutions and defects involving crystal systems, ionization/dissociation of ionogenic groups on the surface of a solid and unequal dissolution of ions on the surface of solid (Feng, *et al*., 2013). In line with the objective of the present paper, the mechanism of interest is where surface charge development occurs by pH induced protonation or deprotonation of surface hydroxyl functional groups (Kosmulski, 2009). The following reactions sum up the surface charging reactions for oxides below and above the point of zero charge pH, which is the pH at which the net surface charge of the solid is zero (Benjamin *et al*. 2015):

Below the point of zero charge pH

The silanols will undergo the following protonation reaction due to pH change

$$\equiv MOH + H^{+} \leftrightarrow MOH_{Z}^{+} \tag{5}$$

Above the point of zero charge pH, the reaction is given as:

$$\equiv MOH + \leftrightarrow MO^{-} + H^{+} \tag{6}$$

In Eq. (5) and Eq.(6), $\equiv MOH$ is a neutral surface species, $\equiv MO^{-}$ is a deprotonated surface site species, $\equiv MOH_{Z}^{+}$ is a protonated surface site species, H^{+} is hydrogen ion and M is a metal.

Accordingly, positive charge develops below the point of zero charge pH while negative charge develops above the point of zero charge pH. Following the development of surface charge, the surface charge density of the solid is quantified as the total charge on the surface per unit area and it depends on the number density of surface functional groups (Zhuralev, 1987) as well as on the specific surface area of porous materials (area per unit mass or per unit pore volume) (Suvachittanont & Tanthapanicchakoon, 1996). In addition to being responsible for the evolution of surface charge densities on solids surfaces, protonated and deprotonated surface sites of solids in contact with aqueous media of varying ionic strength also contribute electron acceptor and electron donor components of solid-liquid interfacial tensions within the framework of intermolecular forces contribution to interfacial phenomena,. These species (electron donor and electron acceptor species) are pH dependent through the following equation (Glover *et al*., 1994):

$$R_{pH}^{-} = \frac{\left[H^{+}\right]_{pzc}^{2}}{\left[H^{+}\right]_{pzc}^{2} + \left[H^{+}\right]^{2}} \tag{7}$$

$$R_{pH}^{+} = 1 - R_{pH}^{-} = \frac{\left[H^{+}\right]_{pzc}^{2}}{\left[H^{+}\right]_{pzc}^{2} + \left[H^{+}\right]^{2}} \tag{8}$$

In this equation, R_{pH}^{-} is the fraction of surface sites available for adsorption of positively charged species [-], R_{pH}^{+} is the fraction of surface sites available for the adsorption of negatively charged species[-], $\left[H^{+}\right]$is hydrogen ion concentration [M], $\left[H^{+}\right]_{pzc}$ is hydrogen ion concentration at the point of zero charge pH [M].

In the following section, we will explain the contributions of charged surface sites expressed by Eq. (7) and Eq. (8) to solid-liquid interfacial tension.

2.4 Soli-Liquid Interfacial Tension and its Thermodynamic and Equation of State Models

The solid-liquid interfacial tension /free energy is the thermodynamic work required to increase the interfacial area under isothermal conditions. While the fluid-fluid interfacial tension has been well studied and characterized, many challenges still remain regarding that of the solid-fluid interface. Two reasons have been cited for these challenges Drecher *et al*., (2018)**.** First, there is anisotropic possibility of the solid, which leads to an imminent difference between surface free energy and surface stress tensor in light of the Shuttleworth effect. The second reason has to do with methodology, where the effects of parameter settings on a simulation work are unknown. On the contrary, several approaches have appeared in the literature for determining solid-liquid interfacial tension. Drecher *et al*., (2018) presented a statistical approach that consists in running a series of molecular simulations of similar systems with different initial conditions, leading to a distribution of surface tensions from which an average value and uncertainty can be extracted. A method based on the concept of excess free energy, invoking the Lennard Jones system in a molecular dynamic simulation work has been presented (Mezei, 1989). The equation of state approach has also been published (Zhu *et al*., 2007). However, of particular interest to us in this paper is the thermodynamic model of solid-liquid interfacial tension that integrates intermolecular forces theory. In this regard, the equation of Oss *et al*., (1988) will be pursued because of the direct relationship between solid-liquid interfacial tension components and aqueous solution pH dependency. The equation of Oss *et al*., (1988), gives the relationship between the interfacial tension between a solid and a liquid as:

$$\gamma_{SL} = \left(\left(\gamma_S^{LW}\right) - \left(\gamma_L^{LW}\right) + 2\left(\left(\gamma_S^{+}\gamma_S^{-}\right)^{0.5} + \left(\gamma_L^{+}\gamma_L^{-}\right)^{0.5} - \left(\gamma_S^{+}\gamma_L^{-}\right)^{0.5} - \left(\gamma_S^{-}\gamma_L^{+}\right)^{0.5}\right)\right) \tag{9}$$

In light of Equation (5) and Eq. (6), the electron donor and electron acceptor components of Eq. (9) originate from deprotonation and protonation reactions respectively of surface silanols groups, these reactions being related to amphoteric surfaces in nature and pH dependent.

2.5 Computed and Experimental Trends in Solid-liquid Interfacial Tension Variation With pH

In view of the pH dependence of the polar contributions to Solid-liquid interfacial tension due to the pH dependent nature of amphoteric surfaces in contact with liquids, a graphical relations between solid-liquid interfacial tension variations with pH has been presented in the literature. Vitoz *et al*., (1998) have given a theoretical plot of solid-liquid interfacial tension versus pH of aqueous solution. Figure 2 shows the plot.

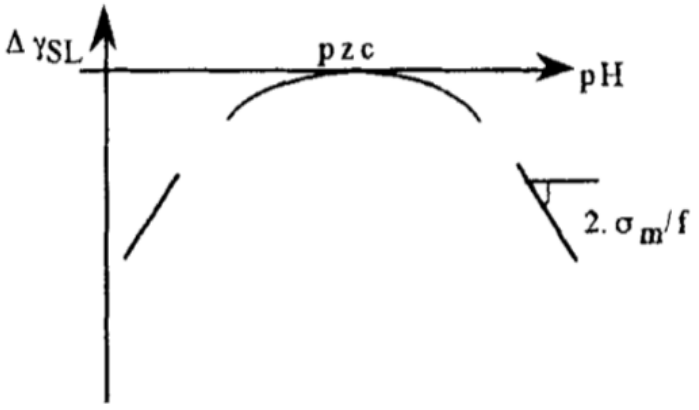

Figure 2. Theoretical plot of solid-liquid interfacial tension versus pH of aqueous solution (Vitoz *et al*., 1998)

Barrancor Jr .*et al*., (1997) have given experimental plot of solid liquid interfacial tension versus pH. Figure 3 shows the plots for a pH range for the point of zero charge pH of silica ranging from 3 to 7.

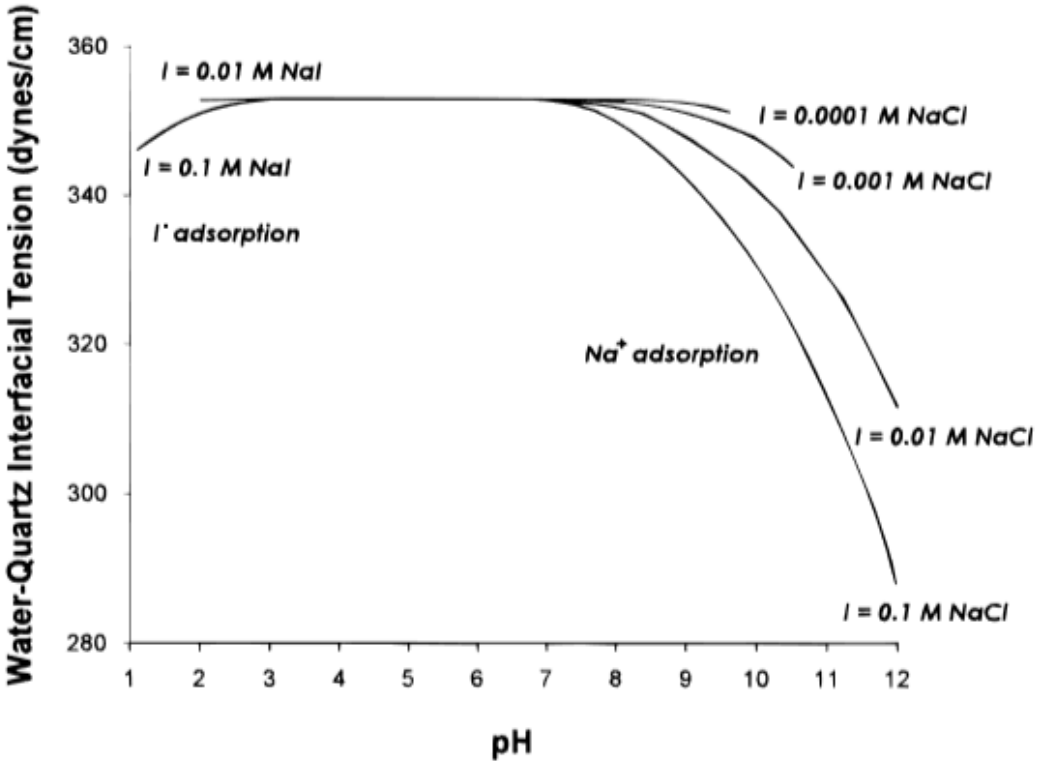

Figure 3. A plot of solid-liquid interfacial tension versus pH (Barrancor Jr *et al*., 1997)

2.6 The thermodynamic Contact Angle and Its Relationship to Other Contact Angles

At the point of contact involving a solid and two fluid phases, the application of mechanical equilibrium to interfacial stresses or tensions between individual phases, assuming a mechanical equilibrium leads to an equation that links the cosine of the contact angle to the ratio of interfacial tensions. This is Young's equation and it is valid for conditions of thermodynamic equilibrium involving the phases in contact. Strictly speaking, Young's equation calculates contact angles for ideal cases relating to solids, where there is no contact angle hysteresis (Gao and McCarthy, 2006) or surface heterogeneities. In cases where there are surface roughness and surface heterogeneities, the contact angle involved cannot be equated to Young's contact angle. In such cases, the concept of apparent contact angles is invoked. By regarding a small displacement of the contact line, derivation of surface free energy change leads to a relationship between Young's equation and the apparent contact angle (Jos é Bicoa, 2002). If the surface roughness is quantified, then a rigorous mathematical derivation leads to change in free energy per unit length. By considering change in surface free energy due to the displacement involved in the mathematical analysis, a link between the apparent contact angle and the thermodynamic or Young's contact angle is possible in terms of the surface roughness. This contact angle is Wenzel's contact angle. In the context of the present paper, the thermodynamic contact angle will be pursued both theoretically, in addition to its reported experimental trends in geologic systems for carbon geosequestration.

Like the solid-liquid interfacial tension (Section 2.5), the pH dependence of the thermodynamic contact angle occurs in the literature. In this regard, (Barrancor Jr *et al*., 1997; Trevino *et al*., 2011; McCafferty *et al*., 1997; Orumwense, 1998) have fitted experimental data to contact angle versus pH data. Figure 4 shows plot for experimental data from Orumwense (1998).

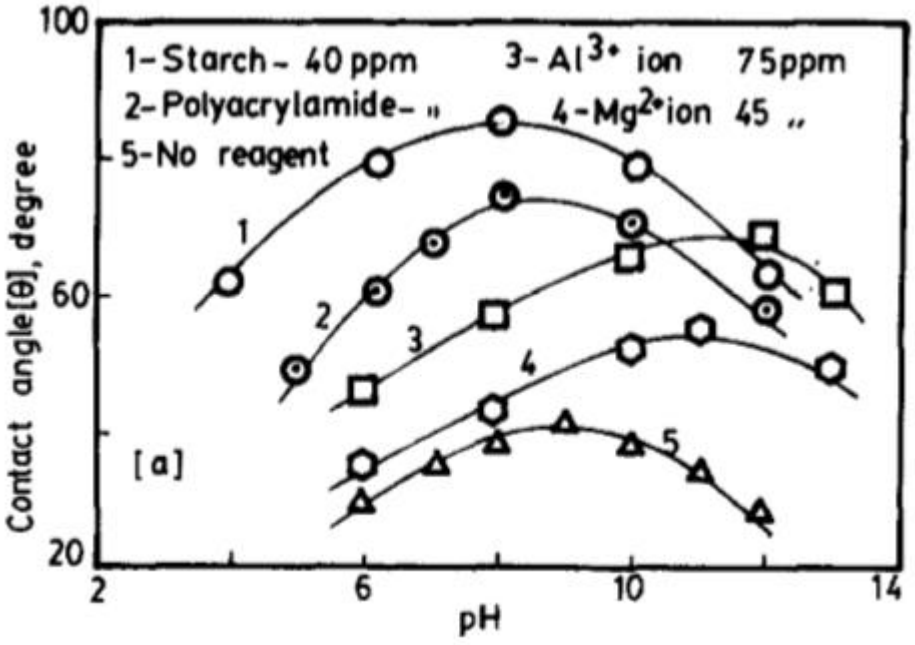

Figure 4. Contact angle versus pH of aqueous solution (Orumwense, 1998)

3. Theoretical Details

3.1 Derivation of pH Dependent Solid-Liquid Interfacial Tension and the Thermodynamic Contact Angle From Surface Charge Regulation Concepts

The dependence of the solid-liquid interface on the pH of an aqueous solution is directly linked to the contributions from acid–base equilibria (Petelska & Figaszewski, 2000). Silica, for instance, will be in various acid–base equilibria with the aqueous medium. The equilibria depends on the pH of aqueous solution relative to the point of zero charge pH and can be described by Eq. (5) and Eq. (6) (Section 2.3), for the case where hydrogen and hydroxyl ions are the potential determining ions in solution. Under such a surface charge regulation, the effective solid-liquid interfacial tension will be the excess Gibbs energy of the solid-liquid interface.

Positive and negative charge sites on the solid surface in contact with an aqueous solution will lead to surface complexation through adsorption of positive aqueous species by negatively charged sites and the adsorption of negative aqueous species by positively charged sites. At the solid-liquid interface, the adsorption will result in a change in solid-liquid interfacial tension in accordance with Gibbs equation given as (McCafferty & Wightman, 1997):

$$d\gamma_{sl} = -RT\sum_i \prod_i \ln(\alpha_i) \tag{10}$$

In this equation $\gamma_{sl}, \Gamma_i, R, T, \alpha_i, \sum_i$ are change in solid-liquid interfacial tension or energy [J/m^2], surface excess adsorption for species i [moles*m^{-2}], universal gas constant [J/K*mole], thermodynamic temperature, activity of species i in solution and summation over all species respectively.

The derivation of Eq. (10) under isothermal conditions was possible, applying Gibbs equation for linking change in interfacial tension to the product of entropy change and temperature change and the product of surface excess and chemical potential (Berg, 2009) as well as the thermodynamic definition of chemical potential (Trinh *et al*., 2015).

Using the theory of logarithm Eq. (10) can be written as:

$$d\gamma_{sl} = -2.3RT\sum_i \prod_i d\log(\alpha_i) \tag{11}$$

In a system where hydrogen and hydroxide ions are the only aqueous species in solution, the surface charge, σ, may be considered as resulting simply from the adsorption of protons (H^+) if the solid surface is negatively charged and from the adsorption of OH^- if the solid surface is positively charged (Chau & Porter, 1991). However, for a multispecies aqueous solution, the surface charge results from the adsorption of different species at the interfacial sites of opposite charges. Consequently, Parks (1984) suggested the computation of solid-liquid interfacial tension applying a numerical approach to Eq. (11). For a geologic system where a solid/rock surface is in contact with an aqueous solution such as formation fluid or brine, the change in solid-liquid interfacial tension will be due to changes in the activity of hydrogen ions, such changes being directly due to the encroachment of hydrothermal fluids (Sedwick & Goff, 1994), magmatic activities (Lowenstern, 2001) or the direct injection of anthropogenic carbon dioxide into saline aquifers (Michael & Aiken, 2010). Consequently, Eq. (11) can be written without the summation as:

$$d\gamma_{sl} = -2.3RT\Gamma_{H^+} d\log\left[H^+\right] \tag{12}$$

In which Γ_{H^+} is the surface excess adsorption for hydrogen ion [moles/m^2]

Under that condition, change in solid-liquid interfacial tension given by E. (12) will be due solely to change in hydrogen ion activity. Using the chemical definition of pH (Bates, 1948) Eq. (12) becomes:

$$d\gamma_{sl} = 2.3RT\Gamma_{H^+} dpH \tag{13}$$

Equation (13) gives a direct relationship between sold-liquid interfacial tension change and pH change of aqueous solution in contact with the solid. Positively and negatively charged sites described by Eq. (7) and Eq.(8) respectively will be responsible for surface charge densities (Benjamin *et al*., 2015). The surface charge density, which is measured as the product of surface excess in moles per area and Faraday constant will be described by the following equation, for surface complexation reactions through hydrogen ion adsorption by negatively charged sites above the point of zero charged pH:

$$\sigma = \Gamma_{H^+} F \tag{14}$$

In which σ is the surface charge density [Cm^{-2}] and F is Faraday constant [C/mole]

Literature reviews show that a simple thermodynamic analysis of adsorption and desorption reactions of protons permits relating change in solid-liquid interfacial free energy to the surface charge density of the interface (McCafferty & Wightman, 1997; Chau & Porter, 1991). Consequently, putting together Eq. (13) and Eq. (14) leads to the following equation:

$$d\gamma_{sl} = 2.3RT\frac{\sigma}{F} dpH \tag{15}$$

Equation (15) gives the relationship between solid-liquid interfacial tension change and pH change of aqueous solution, where the surface charge density of the solid is another variable. For a three-phase system of solid-liquid-gas or solid-liquid-liquid, the three-phase contact line will result in a thermodynamic contact angle or Young's contact angle. Assuming there is no dissolution or swelling following solid-liquid interaction, for a solid-liquid-gas system, the relationship between contact angle and individual interfacial tensions is given by Young's equation as (Makkonen, 2016):

$$\gamma_{\mathrm{lg}} \cos\theta = \gamma_{sg} - \gamma_{sl} \tag{16}$$

In which γ_{lg} [Nm^{-1}] is liquid-gas interfacial tension, γ_{sg} is solid-gas interfacial tension [Nm^{-1}], γ_{sl} sold-liquid interfacial tension [Nm^{-1}] and θ is the contact angle.

Assuming the solid-gas interfacial tension is constant (Zhu *et al.*, 2007) and the liquid gas interfacial tension is also constant, taking the differential of Eq. **(**16**)** gives:

$$\gamma_{\lg} d\cos\theta = -d\gamma_{sl} \tag{17}$$

Equation (17) was deduced based on the constancy of interfacial tension when hydrochloric acid or sodium hydroxide is used to effect pH changes (Vitoz *et. al*., 1998).

Putting together Eq. (16) and Eq. (17) leads to the following equation:

$$d\cos\theta = -2.3RT\frac{\sigma}{F\gamma_{ig}}dpH \tag{18}$$

Equation (18) gives the relationship between contact angle change and the pH change of an aqueous solution. At this point, reference to Eq.(7) and Eq.(8) shows that the surface charge density, positive below the point of zero charge pH and negative above the point of zero charge pH, is pH dependent (Kosmulski , 2011). Also, by electrostatic theory, a given surface charge density will give rise to a surface potential (Horiuchi, *et al*, 2012).

The mathematical relationship between surface charge density and interfacial electrostatic potential is often derived based on the concept of condensers of constant capacitance (Kallay *et al*., 2010). Using the relationship between surface charge density and surface potential (Atkinson *et al*., 1967) the following can be written:

$$\frac{e\psi}{k_B T} = \sigma\left(\frac{2\pi}{\varepsilon n k_B T}\right)^{-0.5} \tag{19}$$

In which σ [Cm^2] is the surface charge density, ε is the dielectric permittivity [Fm^{-1}], ψ is the surface potential [V], T is the thermodynamic [K], n is the number density of ions [m^{-3}], k_B is Boltzmann's constant [JK^{-1}], e is the electronic charge [C] and π is equal to 3.14.

Thus:

$$\sigma = \left(\frac{2\pi}{\varepsilon n k_B T}\right)^{-0.5}\frac{e\psi}{k_B T} \tag{20}$$

Substitution of charge density from Eq. (19) into Eq. (15) and Eq. (18) gives:

$$d\gamma_{sl} = 2.3RT\frac{\varepsilon\kappa\psi}{F}dpH \tag{21}$$

$$d\cos = -2.3RT\frac{\varepsilon\kappa\psi}{F\gamma_{\lg}}dpH \tag{22}$$

Based on the fundamental concept of the two-step protonation reactions or the 2-pk model (Plasecki *et al*., 2001; Lutzenkirchen, 1998) **(Plasecki, Rudzinski, & Charmas, 2001)**, the following equation can be derived **(**Preocanin *et al*.**,**2006**)**.

$$\psi = \frac{RT\ln(10)}{2F}\log\left(K_1^0 K_2^0\right) - \frac{RT\ln(10)}{2F}\log\left(\frac{\{MOH_2^+\}}{\{MO^-\}}\right) - \frac{RT\ln(10)}{F}pH \tag{23}$$

In which K_1^0 is the first ionization constant for deprotonation of a surface functional group [M] and K_1^0 is the second ionization constant for protonation of a surface functional group [M^{-1}], all other terms have already been explained.

Invoking the concept of point of zero charge pH of solid surface (Lyklema, 1984; Sposito, 1998; Sonnefeld, 2001) the following can be written:

$$2pH_{pzc} = \log\left(K_1^0 K_2^0\right) \tag{24}$$

Substitution into Eq. (23) into Eq. (23) gives:

$$\psi = \frac{RT\ln(10)}{F}\left(pH_{pzc} - pH\right) - \frac{RT\ln(10)}{2F}\log\left(\frac{\left\{MOH_2^+\right\}}{\left\{MO^-\right\}}\right) \tag{25}$$

Equation (25) can also be written as:

$$\psi = \frac{RT\ln(10)}{F}\left(pH_{pzc} - pH\right) + \frac{RT\ln(10)}{2F}\log\left(\frac{\left\{MO^-\right\}}{\left\{MOH_2^+\right\}}\right) \tag{26}$$

The following practical interpretations can be made regarding Eq. (25) and Eq. (26):

In Eq.(25), the second term on the right handside must be zero above the point of zero charge pH of the solid surface because protonated surface species are non existent. Similarly, in Eq. (26), the second term on the right hand side must be zero below the point of zero pH of the solid surface because depronated species are non existent. Hence, using the two-step protonation theory, the following can be written to represent surface potential:

$$\psi = 2.303\frac{RT}{F}\Delta pH \tag{27}$$

The pH change in Eq. (27) is the one measured relative to the point of zero charge pH.

Thus,

$$\psi = \frac{2.3RT}{F}\left(pH_{pzc} - pH\right) \tag{28}$$

Substitution for surface potential from Eq. (28) into Eq. (20) gives:

$$\sigma = \left(\frac{2\pi}{\varepsilon n k_B T}\right)^{-0.5}\frac{e}{k_B T}\frac{RT\ln(2)}{F}\left(pH_{pzc} - pH\right) \tag{29}$$

Substitution of Eq. (29) into Eq. (21) and Eq. (22) gives:

$$d\gamma_{sl} = 2.3RT\frac{2.3^2R^2T^2}{F^2k_BT}\left(\frac{2\pi}{\varepsilon n k_B T}\right)^{-0.5}\left(pH_{pzc} - pH\right)dpH \tag{30}$$

$$d\cos\theta = -2.3RT\frac{2.3^2R^2T^2}{F^2k_BT\gamma_{\lg}}\left(\frac{2\pi}{\varepsilon n k_B T}\right)^{-0.5}\left(pH_{pzc} - pH\right)dpH \tag{31}$$

The equations can be written for a solid-liquid-liquid system as well. Equation (30) and Eq. (31) link solid-liquid interfacial tension change and change in cosine of contact angle to the pH change of aqueous solution respectively. To develop explicit equations relating them (solid-liquid interfacial tension and cosine of contact angle) to the pH of aqueous solution individually requires direct integration of each differential equation. Following Vitoz *et al* (1998), solid-gas interfacial tension will be assumed constant where pH changes are caused by hydrochloric acid or sodium hydroxide solution. A correlation exists between surface tension and dielectric permittivity (Holmes, 1973). Therefore, if surface tension is assumed constant, dielectric permittivity will also be constant and so will the number density of ions in solution, in view of the dependence of dielectric permittivity on ionic concentration (Stogryn, 1971). Integration, using the point of zero charge pH as the lower limit and the pH of the aqueous solution as the upper limit leads to the following equations:

$$\gamma_{sl} = \gamma_{sl}^{pzc} + A + \zeta pH + \xi pH^2 \tag{32}$$

$$\cos\theta = \cos_{sl}^{pzc} + B + \lambda pH + \omega pH^2 \tag{33}$$

Where,

$$A = -0.5\beta pH_{pzc}^2$$

$$\zeta = \beta pH_{pzc}$$

$$\xi = -\beta 0.5$$

$$B = 0.5\beta pH_{pzc}^2 \tag{34a}$$

$$\lambda = -\beta pH_{pzc}$$

$$\omega = 0.5\beta$$

and

$$\beta = 2.3RT\frac{\varepsilon\kappa}{F}\frac{2.3k_BT}{e} \tag{34b}$$

Hence,

$$\gamma_{sl} = \eta + \zeta pH + \xi pH^2 \tag{35}$$

$$\cos\theta = \mu + \lambda pH + \omega pH^2 \tag{36}$$

Where,

$$\eta = \gamma_{sl}^{pzc} + A$$

$$\mu = \cos_{sl}^{pzc} + B \tag{37}$$

Equation (35) and Eq. (36) show quadratic trends. The validation of Eq.(36) will be pursued in the appropriate section.

3.3 Modelling the Effect of Salinity on Surface Charge Density at a Given pH

In line with our objective in this paper, we will limit ourselves to the case of geological carbon storage (Bachu & .Adams, 2003), where anthropogenic carbon dioxide is injected into a saline aquifer for long term immobilization through the process of dissolution and formation of stable carbonates (Soong *et al*., 2004). We will assume the cases of sandstone saline aquifers proven to have the greatest promise for storage capacity; with a single aquifer, (Mt. Simon Sandstone), in North America having 94 (Andersen, 2017) Gt storage capacity. For such a system, the solubility of injected carbon dioxide will depend on salinity and pressure (Portia & Rochelle, 2005). Dissolved gas in formation brine will hydrate to give carbonic acid, which will dissociate to give bicarbonate and hydrogen ions (Espinoza &

Santamarina, 2010). Consequently, for a given salinity of sodium chloride solution in contact with carbon dioxide at a given pressure and temperature, the total surface sites of surface silanol will be given as:

$$\sigma = \Gamma_{Tot} = \left[\{SiOH\} + \{SiOH_2^+\} + \{SiOH_2^+ \cdot Cl\}\{SiOH_2^+ HCO_3^-\} + -\{SiO^-\} - \{SiO^- \cdot Na\} + \{SiO^- H^+\}\right] \quad (38)$$

In which Γ_{Tot} is the total surface sites density [moles m^{-2}], $\{SiOH_2^+ \cdot Cl\}$ are protonated surface sites complexed by chloride ions [moles m^{-2}], $\{SiOH_2^+ \cdot HCO_3^-\}$ are protonated surface sites complexed by bicarbonate ions [moles m^{-2}], $\{SiO^- \cdot H^+\}$ are deprotonated surface sites complexed by hydrogen ion adsorption [moles m^{-2}] and $\{SiO^- \cdot Na\}$ are deprotonated surface sites complexed by sodium ions [moles m^2].

The resulting surface charge density is computed as:

$$\sigma = F\Gamma_{Tot} = F\begin{bmatrix} \{SiOH\} + \{SiOH_2^+\} + \{SiOH_2^+ \cdot Cl\}\{SiOH_2^+ HCO_3^-\} + -\{SiO^-\} - \{SiO^- \cdot Na\} \\ + \{SiO^- H^+\} \end{bmatrix} \quad (39)$$

Above the point of zero charge pH, protonated surface sites don not exist. Therefore, the surface charge density can be written as:

$$\sigma = F\Gamma_{Tot} = F\left[\{SiOH\} - \{SiO^-\} - \{SiO^- \cdot N_a^+\} - \{SiO^- H^+\}\right] \quad (40)$$

Similarly, below the point of zero charge pH, negative surface sites do not exist and surface charge density computation gives:

$$\sigma = F\Gamma_{Tot} = F\left[\{SiOH\} + \{SiOH_2^+\} + \{SiOH_2^+ \cdot Cl\} + \{SiOH_2^+ HCO_3^-\}\right] \quad (41)$$

All the species defined by Eq. (39) through Eq. (41) are pH dependent.

In line with our principal objective of providing theoretical explanations for the physicochemistry of wetting related to silica systems associated with geological carbon storage, we will, at this point, limit ourselves to the formation of surface complexes associated with deprotonated surface sites of silanols (Eq. (40)). The reason is that, recent studies (Gilfillan *et al*, 2009) have shown that the minimum pH for a natural ideal carbon dioxide system related to natural gas reservoirs due to solubility trapping is 5, which is above the point of zero charge pH of silica (3 on the average, Kosmulski, 2002) surface or the effective point of zero charge pH of sandstone aquifers that have subordinate amounts of other minerals (Huang, 1962).

Following Andrea *et al*., (2017) an equilibrium constant K, can be related to reactants and products as:

$$K\{\equiv SiO^-\}\{N_a^+\}\{H^+\} = \{\equiv SiO^- \cdot N_a^+\}\{\equiv SiO^- \cdot H^+\} \quad (44)$$

Thus:

$$\{\equiv SiO^- \cdot N_a^+\} = \frac{K\{\equiv SiO^-\}\{H^+\}\{N_a^+\}}{\{\equiv SO^- H^+\}} \quad (45)$$

Substitution of Eq. (45) into Eq. (40) gives:

$$\sigma = F\Gamma_{Tot} = F\left[\{SiOH\} - \{SiO^-\} - \left[\frac{K\{\equiv SiO^-\}\{H^+\}\{N_a^+\}}{\{\equiv SiO^- \cdot H^+\}}\right] - \{SiO^- H^+\}\right] \quad (46)$$

The first ionization constant of the 2-pk model is related to reactant and products as:

$$\{\equiv SiOH\} = \frac{\{\equiv SiO^-\}\{H^+\}}{K_1} \tag{47}$$

Substitution of Eq. (47) into Eq. (46) gives:

$$\sigma = F\Gamma_{Tot} = F\left[\frac{\{\equiv SiO^-\}\{H^+\}}{K_1} - \{SiO^-\} - \left[\frac{K\{\equiv SiO^-\}\{H^+\}\{N_a^+\}}{\{\equiv SiO^- \cdot H^+\}}\right] - \{SiO^-H^+\}\right] \tag{48}$$

Using functional notation, the following can be written:

$$\sigma = \sigma\left(\equiv \{\equiv SiOH\}, \{\equiv SiO^-\}, \{SiO^-H^+\}, \{H^+\}, \{N_a^+\}\right) \tag{49}$$

Equation (48) links surface charge density above the point of zero charge pH of silica surface to several species. Among the species, the one responsible for negative surface density and potential is the deprotonated surface site silanol occurring in the first, second and third terms on the right hand side of the equation. The implications of Eq. (40), Eq. (41) and Eq. (48) for surface charge densities above and below the point of zero charge pH respectively will be discussed in the appropriate section.

3.4 Validation of Models

3.4.1 Validation of Contact Angle Versus pH Equation

Validation of any of our models requires experimental data on solid-liquid interfacial tension or cosine of contact angle versus pH. Where experimental data are not generated, data from literature sources require information about key parameters of the systems such as the point of zero charge pH of solid surface as well as the value of the parameter in question (solid-liquid interfacial tension or cosine of contact angle) at the point of zero charge pH of solid surface. Carre *et al*., (2003), have published experimental plot of contact angle versus the pH of aqueous solution. They used deionized water at room temperature, where dilute hydrochloric acid was used to change pH. In the cited experiment, the volume of water used was 2 microliters and the resistivity was measured as 18 Ohcm. To calculate the number density of ions, we used a pH value of 6.998 corresponding to a resistivity of 18.15 Ohcm (Light & Licht, 1987) at room temperature. To calculate the number density, we calculated the number of moles of hydrogen and hydroxyl ions per liter at the given pH. Next, we calculated the actual number of ions present in 2 microliter of experimental water multiplying the total ionic concentration by Avogadro's number. To obtain the number density in number per cubic meter, we divided the result by 0.001 m^3 per liter.

To validate our model that links the cosine of the thermodynamic contact angle to the pH of aqueous solution, Table 1 below shows the parameters taken from literature sources to calculate the coefficient, β , of our equation Eq.(33).

Table 1. Parameters for calculation of coefficient (β)

Parameter	Value	Reference
Thermodynamic temperature standard condition) (K)	298	(Brady & Walther, 1989)
Faraday constant (C $mole^{-1}$)	96485.33	(NIST, 2015)
Surface tension of deionized water, γ_{lg} (Nm^{-2})	71.99	(Heller *et al.*, 1966)
Permittivity of deionized water, ε (Fm^{-1})	78.54	(Maryott & Smith, 1951)
pH_{pzc}	7.3	Carre *et*., *al* (2003)
pH of experimental water	6.998	(Light & Licht, 1987)
Avogadro's number ($mole^{-1}$)	$6.02*10^{23}$	(Mohr & Taylor, 1998)
Universal gas constant (J/mole*K)	8.3 J/mole	(Mohr & Taylor, 1998)
Electronic charge (C)	$1.6*10^{-19}$	(Mohr & Taylor, 1998)
Boltzmann constant (J/K)	$1.83*10^{-23}$	(Mohr & Taylor, 1998)
Avogadro's number (mol^{-1})	6.022*1023	(NIST, 2015)

Table 2. Comparison of calculated parameters (coefficients) of our model (Eq. (31) to those of literature values (Carre *et al*., 203)

Parameter	Results Calculated	Value from experimental data Carre *et al*., (2003)	Difference
Mu	0.7400	0.7084	0.0316
Omega	0.0037	0.0031	0.0006
Lamda	-0.0539	-0.0451	-0.0088

Based on the calculated coefficients, the following equation can be written to describe trend in experimental data obtain by Carre *et al*., (2003):

$$\cos\theta = 0.7400 - 0539\,pH + 0.0037\,pH^2 \tag{50}$$

The fitting equation is given as (See Appendix 1-Carre *et al*., 2003):

$$\cos\theta = 0.7084 - 0.0451pH + 0.0031pH^2$$

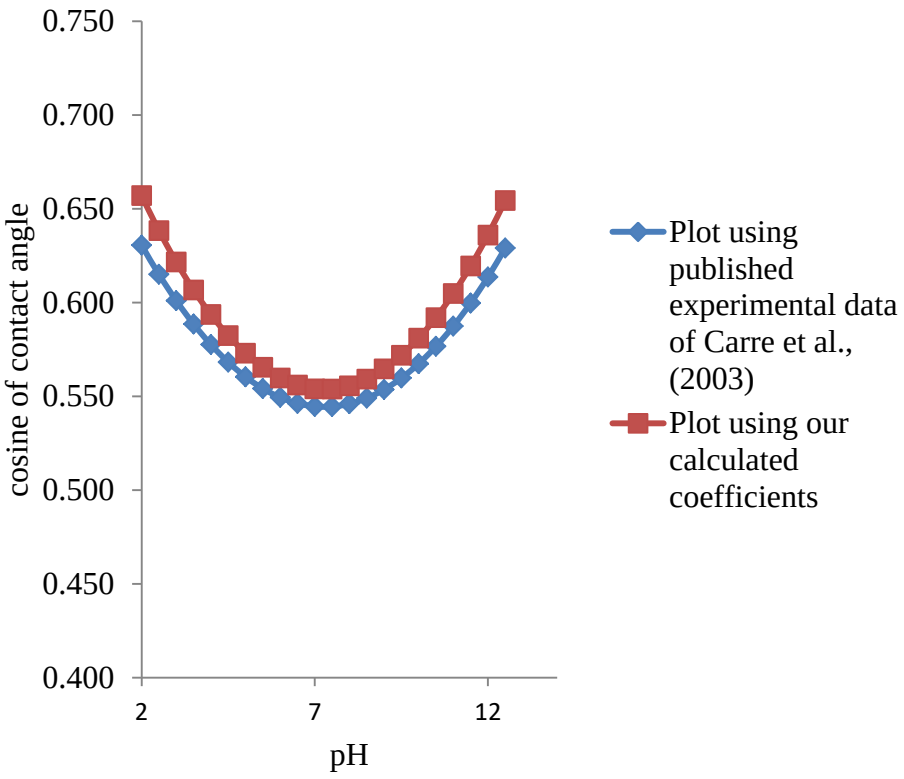

Figure 5. Comparison of cosine of contact angle versus pH plot using or model to that based on experimental data of Carre *et al*., 2003

In the derivation of the pH dependent solid-liquid interfacial tension, Young's equation, which considers mechanical equilibrium taking into consideration the three-phase contact line, was invoked. Therefore, the thermodynamic contact angle, which does not integrate the effect of roughness (Long et al., 2005) is implied.

Rimstidt (Rimstidt, 2015) examined the data compiled from literature by Dove (Dove, 1994) and Bickmore *et al*., 2008) for 285 dissolution experiments in acid and alkaline solutions between pH values of 1 and 12 and at temperatures ranging

from 25 ^{o}C to 300 ℃. He correlated these data using an empirical regression that shows the effect of acid and alkaline on silica dissolution rate (Rimstidt, 2015). The regression shows that silica dissolution increases with decrease in pH and increases with increase in pH. At high pH, where SiO_2 surface sites are deprotonated and therefore carry negative charge, detachment of silicon appears to control the overall silicate dissolution rates. At low pH, near the zero point of charge of SiO_2 (where surface charge is dominated by the other oxide components), detachment of the non-silicon structure-forming oxides apparently control dissolution rates. (Brady & Walther, 1989). Regarding Figure 5, the deviation our or model prediction from experimental data can be explained as follows:

In line with the regression findings of (Rimstidt, 2015), we expect silica dissolution to increase as pH increases away from the point of zero charge pH. The implication is that increase surface roughness due to dissolution will cause experimentally measured contact angles to differ from those predicted by our model. The trend also holds true for decrease in pH away from the point of zero charge pH. Consequently, significant deviation of our model from experimental data is expected as pH decreases and increases away from the point of zero charge pH and this is clearly seen in Figure 5.

3.5 Thermodynamic Validation of pH versus Contact Angle Model using Pressure versus Contact Angle Data

To validate our model (Eq. (36)) in the thermodynamic context, we noticed that the solubility of carbon dioxide is a function of salinity and temperature (Mohammadian *et al.*, 2015), and that a plot of contact angle versus pressure must also give a parabolic trend like that of contact angle versus pH. What is more, there is a correlation between hydrogen ion concentration and the pH of an aqueous solution (Bain *et al*., 1989). Consequently, using solubility data versus pressure at a given temperature and salinity of aqueous solution enables conversion of hydrogen ion concentration versus pressure data to pH versus pressure data due to the dissociation of hydrated species of carbon dioxide in accordance with the following equation (Millero *et al.* 2002).

$$K_1 = \frac{\left[H^+\right]\left[CHO_3^-\right]}{\left[CO_2\right]} \tag{51}$$

In which K_1 is the first dissociation constant of carbonic acid [M], $\left\|H^+\right\|$ is the hydrogen ion concentration [M], $\left[CHO_3^-\right]$ is the concentration of bicarbonate ions [M] and $\left[CO_2^*\right]$ is the concentration of the hydrated species of carbon dioxide (carbonic acid) [M].

Therefore, per equation Eq. (51), when dissolved carbon dioxide is hydrated to carbonic acid, one mole of the acid dissociates to give 1 mole of hydrogen ions and one mole of carbonate ions. Based on this equation, hydrogen ion concentration at a given pressure and temperature can be calculated.

Jafari *et al*. (2018), studied contact angle on mica surface for the system brine-CO_2-mica and plotted contact angle versus pressure for one mole of sodium chloride solution at 318 K. To validate our model (Eq. (36)) the solubility of carbon dioxide in one molar solution of sodium chloride at 318 K as a function of pressure is necessary. We obtained the required solubility data interpolating between pressures of 10 bar and 200 bar and temperatures between 303.15 K and 333.15 K, using Table 4 of Duan and Sun (2003),

To calculate hydrogen ion concentration at a given pressure, salinity (1 M) and temperature (318K), we used the following equation:

$$X_{H^+} = \frac{-K + \sqrt{K_1^2 + 4 * X_{CO_2^*} K}}{2} \tag{52}$$

In this equation, K_1 is the first dissociation constant of carbonic acid as a function of temperature and salinity, taking into consideration pressure effect, X_{H^+} is the concentration of hydrogen ions [M] and $X_{CO_2^*}$ is the concentration of the hydrated species of carbon dioxide [M].

Equation (52) was obtained using the dissociation constant equation (Eq. (51)), assuming the solubility of carbon

dioxide in one molar sodium chloride solution is the aqueous form or carbonic acid concentration.

The carbon dioxide/brine system can be characterized using any of four parameters; namely, pH, total alkalinity, carbon dioxide fugacity and total inorganic carbon species (Millero *et al*., 2002) In this regard, information about the pH of the system can be obtained using knowledge of hydrogen ion concentration, which can be calculated using information about the dissociation constant of carbonic acid formed by hydrated species of dissolved carbon dioxide at a given temperature and salinity. In the literature, several models of the dissociation constant of carbonic acid in brine/sea water have been presented, but laboratory measurements and validations of carbon dioxide solubility in sodium chloride brine over varying temperatures, pressures and salinities have resulted in the following equation for the first dissociation constant of carbonic acid Aissa *et al*., 2015):

$$\ln K_1^* = \frac{-2936978}{T^2} + \frac{17883}{T} - 41.4589 + \left(\frac{1141179}{T^2} - \frac{7220.094}{T} + 13.40776\right) * \sqrt{I} - 1.414245 * I + 0.2677258 * I^{2/3} \quad (53)$$

I , is given as (Solomon, 2001): $I = \frac{1}{2}\sum_{i=1} c_i^2 z_i^2$ (54)

In these equation, K_1^* is the first dissociation constant of carbonic acid or hydrated species of carbon dioxide [M], I is the ionic strength, T is the temperature [K],c_i is the ionic concentration [M], and z_i is the number of charges on the ion.

Using equation (53), we calculated the dissociation constant of carbonic acid as $1.415*10^{-6}$ M. Using the value of calculated dissociation constant and solubility data obtained based on interpolation, we calculated hydrogen ion concentration using Eq. (52). We then calculated pH from hydrogen ion concentration using the chemical definition of pH. We then extracted contact angle versus pressure from Jafari *et al* (2018) work based on their Figure 4 c, See Appendix 6 (experiment at one molar sodium chloride solution at 318 K). The following table sums up interpolation and computation results.

Table 3. Derived contact angel versus pH data using solubility and pressure data

Pressure-MPa	Contact angle-deg.	Solubility M	Hydrogen ion concentration- M	pH
3.5	80.0	0.303	0.00066	3.18
5.0	84.5	0.375	0.00073	4.14
7.2	85.0	0.482	0.00083	3.08
10	64.0	0.618	0.00093	3.03
13.5	44.0	0.788	0.00105	2.98

A plot of contact angle versus pH is seen in Figure 6 while a similar plot is found as Appendix 7

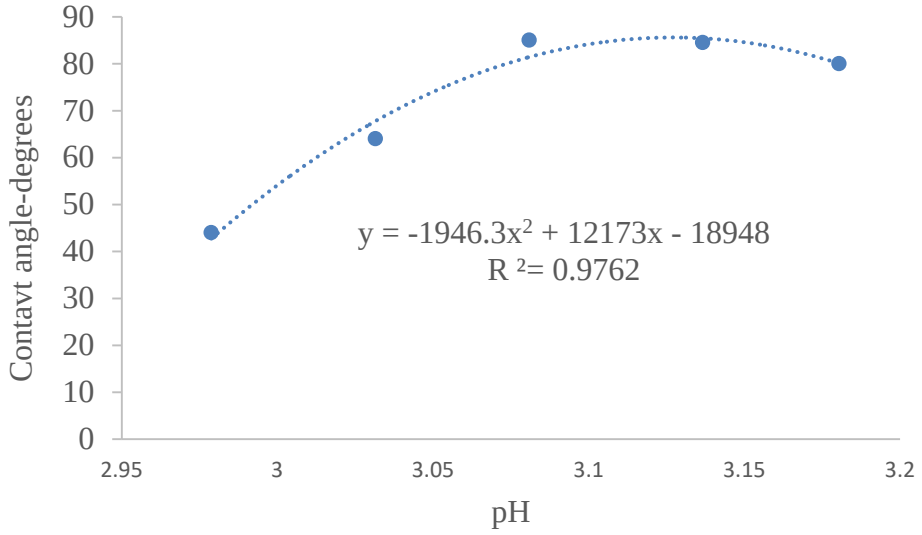

Figure 6. A plot of contact angle versus pH based on Table 3

We will discuss Table 3 and Figure 6 in the following section.

4. Discussion

In the petroleum literature, wettability has been quantified based on wettability index (Amipour *et al*., 2015), which is directly linked to surface energy**.** Consequently, the index of wettability must be equally related to surface energy or interfacial energy between phases. Arsalan *et al*., (2015), have linked wettability index and surface free energies that integrate basic and acidic surface sites of interfacial energy in accordance with the intermolecular forces effect on surface tension and or interfacial tension (Oss *et al*., 1988)**.** The basic and acidic surface sites of solids are pH dependent (Bolland *et al*., 1980). Therefore, the theoretical and fundamental basis of our work are in good agreement with those of Arsalan *et al*., (2015), that link wettability index and pH and we will proceed to discuss our work in some physically meaningful aspects.

Relationship of Our Models to Observed pH Dependent Trends of Solid-Liquid interfacial Tensions and Contact Angle

The importance of surface charge contribution to wettability has been mentioned in diverse fields relating to polymer surface engineering (Hogt, *et al*., 1985) and biological systems (Webb *et al*., 1998). For instance, receding contact angles of methyl methacrylate (MMA) copolymers containing hydrophilic or **charged** units were **decreased** (Hogt, *et al*., 1985) with surface charge increase**.** Also, the importance of double layer repulsion, which draws largely on increased surface charge density (Philipsea *et* al., 2017) and its contribution to disjoining pressure stabilization of the prewetting film has been reported (Joud *et al*., 2013). Simply put, increase in surface charge density or surface potential has been the major factor for wettability enhancement (Park *et al*., 2011; Guo *et al*., 2016). In the field of enhanced oil recovery, many experimental studies have been performed in an attempt to unveil the underlying mechanism behind wettability alteration while zeta-potential measurements have proved that Ca^{2+}, Mg^{2+} and SO_{2-4} are strong potential-determining ions that are strongly related to the surface charge/potential (Liu, *et al*., 2018).

In light of our Eq. (22), the pH derivative of contact angle, which is linked to surface potential, is negative. Consequently, since the surface potential associated with any system increases with surface charge density (Chiu *et al*., 1980), a negative pH derivative implies a decrease in surface charge density. Therefore, regarding Eq. (22), if surface charge density increases wettability (Hogt, *et al*., 1985)**,** then decreasing surface charge density will decrease wettability to increase the thermodynamic contact angle. The implication for a system where pH decreases is that, the derivative becomes a bigger negative value, meaning a decrease in surface charge density and potential, implying an increase in solid-liquid interfacial tension with decrease pH of aqueous solution in contact with the solid. Per Young's equation (Makkonen, 2016), increase solid-liquid interfacial tension, where liquid-air interfacial tension and solid-air interfacial tension remains constant means a decrease in the numerator of the equation and this means decrease in the cosine of the

thermodynamic contact angle, leading to increases contact angle.

Generally, solid-liquid interfacial tension increases with pH decrease and reaches a maximum at the point of zero charge pH (Parks, 1984) and then decreases with pH increase away from the point of zero charge pH in line with Eq. (30). The implication is that decrease pH towards the point of zero charge pH causes hydrogen ion increase, causing protonation of negatively charged surface sites in accordance with Lechatelier's famous principle (Knox, 1985). For the silica-water interface, the reaction is described by Eq. (6) as:

$$\equiv MOH + \leftrightarrow MO^{-} + H^{+}$$

In this equation, M stands for silica.

The gradual protonation reaction with pH decrease, therefore, represents a gradual decrease in surface charge density to cause increase in solid-liquid interfacial tension. A maximum value is reached at the point of zero charge pH, where only neutral surface sites exist or where the net surface charge is zero (Kosmulski, 2009). Similarly, as pH decreases away from the point of zero charge pH, protonation of surface neutral species will occur in accordance with Eq. (5) as:

$$\equiv MOH + H^{+} \leftrightarrow MOH_{Z}^{+}$$

Contrary to protonation of negatively charged sites which causes decrease in surface charge density, the reaction described by Eq. (5) causes increase in surface charge density leading to a gradual decrease in solid-liquid interfacial tension. Therefore, the cosine of the thermodynamic contact angle will also follow a similar trend, decreasing towards the point of zero charge pH and increasing away from the point of zero charge pH (Eq. (36)), with pH increase similar to that observed related to Titania surface, where the static contact angle decreases above and below the point of zero charge pH in a Lippman-like manner as the pH is altered (Pua, *et al*, 2010). Accordingly, the two equations (Eq. (33) and Eq. (36)) , developed in our studies, using surface charge and surface potential dependence on aqueous solution pH theoretically explain the coupling of the thermodynamic contact angle to surface potential and surface charge density (Horiuchi *et al*., 2012).. Therefore, our models ((Eq. (35) and Eq. (36)) explain trends in solid-liquid interfacial tension versus aqueous solution pH or contact angle versus aqueous solution pH respectively.

Equation (49) shows that the surface charge density above the point of zero charge pH is a function of the concentrations of neutral surface site silanols, deprotonated surface sites silanols, surface site complex, hydrogen ions and sodium ions. Accordingly, Eq. (48) shows that the only species on the right hand side that is responsible for surface charge density and potential is the deprotonated surface site silanol ($\equiv SiO^{-}$), with hydrogen and sodium ions occurring as aqueous species while $\equiv SiO^{-}H^{+}$ occurs as a surface site complex. Equation (48) shows that it is possible to keep the salinity (sodium ions) of an aqueous solution constant while varying the remaining parameters; meaning it is possible to investigate the effect of salinity on surface charge density under isothermal conditions. In this case, where pH is the variable, the other species ($\equiv SiO^{-}$, $\equiv SiO^{-}H^{+}$, $\equiv SiOH$) will automatically vary through the pH induced surface charge regulation model (Kosmulski, 2011). Plots of such investigations can be seen in the form of surface charge variation with pH and salinity (Sverjensky, 2005) (See Appendix 5)

Equation (50) represents our model of salinized silica surface used by Carre *et al*., (2003), based on system parameters (point of zero charge pH and cosine of contact angle at the point of zero charge pH of aqueous solution). Generally, our model over calculates the cosine of the contact angle as seen in Figure 5. However, compared to their model using experimental data, we can say that the coefficients of our model based on our theory as seen in Table 2 are quite close to their coefficients. Accordingly, Appendix 2 shows calculated cosine of the contact angle based on our model and that of Carre *et al*., (2003), with fractional errors that are far below 0.1. The fractional error is calculated as the difference between the value calculated using our model and that calculated using Carre *et al*., (2003) model.

Table 3 shows values of pH and contact angle deduced from pressure versus solubility data based on the work of Jafari *et al*. (2018). As pressure increases at a given temperature and salinity, the concentration of dissolved species of carbon dioxide must also increase and this holds true in Table 3. Also, as pressure increases at a given temperature and salinity, hydrogen ion concentration in aqueous solution obtained from the dissociation of carbonic acid must also increase and this holds true as seen in the table.

Per our model of cosine of contact angle/contact angle versus pH, the graph of contact angle versus pH of aqueous solution must be parabolic, with the turning point indicating the maximum contact angle or the minimum cosine of contact angle for graph of cosine of contact angle versus pH. Accordingly, the turning point must coincide with the point of zero charge pH of solid surface. This holds true for our plot as seen in Figure 6. Accordingly, the plot shows a quadratic equation with a very good regression coefficient of 0.98 to 2 decimal places. From Figure 6, the point of zero charge pH of mica surface is 3.15. Appendix 7 from the work of Horiochi *et al*., (2012) shows a similar plot with the maximum contact angle occurring at a pH equal to 2.9 to 3.0, quite in agreement with our value of 3.15. Also, in the work of Kosmulski, (2011), the point of zero charge pH of mica surface has been reported as 3.30, which is quite in agreement with our value.

How Our Model Accounts for the Effect of Salinity on Solid-Liquid Interfacial Tension and Contact Angle

Equation (40) links the surface charge density to surface complexes, where sodium chloride and dissolved carbon dioxide species are the major components of aqueous solution. The justification for considering a predominantly sodium chloride brine stems from Hanor's classifications (Hanor, 1994) scheme, which recognizes a sodium chloride dominated brine. Considering Eq. (40), the second term on the right-hand side is the surface site that will contribute towards surface charge density and surface potential on account of its charged nature. The first term is a neutral surface species while the last two terms are neutralized surface sites. Accordingly, the equation means that, assuming a constant pH, increasing the concentration of sodium ions will cause more complexing of deprotonated surface sites of silanols. The effect will be decreasing surface charge density of deprotonated silanols leading to a net decrease in surface charge density for pH above the point of zero charge pH. Similarly, below the point of zero charge pH Eq. (41) shows that increasing the concentration of chloride and bicarbonate ions will cause more of protonated surface species $\left(\equiv SiOH_2^+\right)$ to be complexed by both ions, causing a decrease in surface charge density, which is due principally to protonated surface silanols $\left(\equiv SiOH_2^+\right)$. Therefore, in line with the relationship between surface charge density and the cosine of the contact angle explained earlier, the net effect of increasing salinity or the concentration of ions in solution is to increase contact angle.

How our Models Account for Observed Trends in Contact Angle versus Pressure in the CO_2-Brine-Silica System

The solubility of carbon dioxide in brine is a function of pressure, temperature and salinity (Portia & Rochelle, 2005). Generally, solubility increases with pressure and decreases with salinity at a given temperature. As pressure increases, the pH of aqueous solution decreases (Espinoza & Santamarina, 2010). Due to increase accumulation of dissolved carbon dioxide species at the interface between carbon dioxide and brine, gas-liquid interfacial tension decreases (Espinoza & Santamarina, 2010).

In recent times, following the drive towards geological carbon storage in saline aquifers as an economically and technically viable option for mitigating global warming, interesting experimental data related to the carbon dioxide-brine-silica system have been published (Kim *et al*., 2012; Chen *et al*., 2016). Kaveh *et al*. (2014), have also studied dewetting of silica surface based on rock samples from the Betheimer sandstone of Germany. In all these research works, contact angles of the said systems were plotted versus carbon dioxide pressure. Obviously, the relationship between pressure and contact angle indirectly simulates the relationship between contact angle and pH, given the pressure dependence of carbon dioxide solubility in brine (Rosenbauer & Koksalan, 2004). Therefore, as pressure increases, increase gas dissolution will result in increased proton concentration via the dissociation of carbonic acid. Accordingly, graphs of contact angle versus pressure in the above cited research works (Kim *et al*., 2012; Chen *et al*., 2016) show contact angle increases with pressure in accordance with our theoretical derivation, where pH decrease corresponds to protonation of deprotonated surface silanols responsible for surface charge density above the point of zero charge pH of silica surface. Kim *et* al., (2012) also plotted pressure versus contact angle for different salinities. They observed that at a given pH of aqueous solution, contacts angles were bigger the higher the salinity. Appendix 3 shows their plots. The salinity effect can be understood from Eq. (48). In this regard, Eq. (48) shows the surface charge density decreases with increases in sodium ions concentration (salinity) and hydrogen ion concentration among others. Therefore, maintaining higher and higher salinities in separate experiments under isothermal conditions while varying pH implies smaller and smaller surface charge densities. The net effect is that plots of contact angle versus pH, which directly correlates with plots of contact angle versus pressure in view of pH dependence on pressure, will show trends where higher salinity curves will be above lower ones. The reason is that for such a system, plots of surface charge or potential versus pH as a function of salinity will show the same trend (Hille *et al*., 1975) (See Appendix 4). Therefore, considering the average pH of experimental brines above the point of zero charge pH of silica (3 on the average) (Kosmulski, 2009), our model (Eq. (48)) satisfactorily explains the observed trend of contact angle versus pressure for varying salinity of aqueous solution. From the electrostatic point of view, Silanol groups on silica surfaces used in the experiments of (Kim *et al*., 2012; Jung and Wan, 2012) in contact with experimental brine at different temperatures and salinities will dissociate, producing hydrogen ions that diffuse away from the surface, leaving pH dependent surface charge and potential. In all cases, pH decreases resulted in two obvious physicochemical processes. They are protonation of negatively charged surface sites on silica surface, assuming the geologic systems are modelled as averagely silica, which decreased surface charge density as well as increase in solid-liquid interfacial tension as already explained. Protonation reaction will be due to the stepwise hydration of carbon dioxide into carbonic acid and ionization into hydrogen and bicarbonate ions (Espinoza & Santamarina, 2010). If solid-gas interfacial tension remains constant, (Zhu *et. al*., 2007) then the numerator of Young's equation decreases. Coupled with decrease liquid-gas interfacial tension, the ratio expressed by Young's equation will decrease. Therefore, in line with wettability enhancement due to increase surface charge density and potential, decrease surface charge density will produce the opposite effect of wetting with characteristic contact angle increase.

In the pressure dependence of pH (Espinoza & Santamarina, 2010), the parabolic trend between the cosine of contact

angle or contact angle and aqueous solution pH given by our model (Eq. (36)) must be seen in the case of contact angle plot versus pressure for a mineral surface. In this regard, Appendix 6 (Jafari & Jung, 2018) shows plots of contact angle versus pressure, with quadratic trends.

However, the quadratic dependence of contact angle on pH may not be strictly realized in the case of actual geological storage conditions due to pH limitation as carbon dioxide dissolves in formation brine. There are three notable limitations. In the first place, hypersaline conditions of saline aquifers could hinder enough dissolution of carbon dioxide in formation brine, which will prevent extreme acidity conditions. Secondly, pH buffering by phyllosilicate minerals due to cation exchange reactions as hydrogen ions from dissolved carbon dioxide are exchanged for exchangeable potassium ions in the octahedral frame works of these minerals (Chapelle & Knobel, 1983). These pH buffering reactions will be associated with clay minerals in aquifer rocks. Dissolution of calcite due to increase hydrogen ions in brine can also cause pH buffering. In the Frio Pilot Scale injection, dissolved carbon dioxide caused calcite dissolution that buffered pH (Kharaka *et al*., 2006). It is also noteworthy that while solubility trapping of injected anthropogenic carbon dioxide is the dominant sink in geological carbon storage, the lowest pH attained has been 5 (Gilfillan *et al*, 2009), which is an obvious limitation to which formation brine pH reduction can enhance geological carbon storage via increasing gas injection sweep efficiency.

Generally, adhesion and wettability behaviour of solids depends on their surface properties, notable among which are roughness, heterogeneity and charge density. Consequently, in many fundamental and technological applications, such as the wetting of oil-reservoir rocks, hydrometallurgical processes involving mineral flotation (Dans *et al*., 2018), electrowetting driven operations (Kan, 2002) and contact angle studies on functionalized surfaces (Hogt, *et al*., 1985), charged surfaces are of prime importance. To understand and predict the wettability a basic understanding of the influence of electrostatics on the interfacial tension of the solid liquid interface is required. In this study, we have used the theory of surface charge dependence of the solid-liquid interfacial tension, based on pH induced surface charge regulation concept to derive a pH dependent solid-liquid tension and a pH dependent cosine of contact. The following sum up the conclusion of our work.

1. Given the concept of pH dependent surface charge regulation and the relationship between surface charge and solid-liquid interfacial tension, a pH dependent solid-liquid interfacial tension can be theoretically derived,
2. Based on the relationship between the cosine of contact angle and the sold-liquid interfacial tension, a pH dependent cosine of contact angle can be theoretically derived, using the relationship between solid-liquid interfacial tension and pH dependent surface charge density,
3. Both pH dependent solid-liquid interfacial tension and pH dependent cosine of contact angle equations satisfactorily explain experimentally observed trends in solid-liquid-interfacial tension and cosine of contact angle variation with aqueous solution pH.
4. It is possible to convert contact angle versus pressure data to contact angle versus pH data for the carbon dioxide-brine-silica system to give a parabolic trend curve typical of the latter.

Acknowledgements

In writing this manuscript, we wish to greatly acknowledge the immense contributions from Dalhousie University Document Delivery service, that made it possible to explore the fundamental bases of our research topic to the depths. The faculty of graduate studies also supported this research to the required extent and we wish to express our gratitude for that. The financial support from the Office af Research and Graduate Studies, Cape Breton University, is also acknowledged.

References

Aissa, M. F., Bahloul, S., Monteau, J. Y., & Alain, L. B. (2015). Effect of Temperature on the Solubility of CO2 in. *International Journal of Food Properties, 18*, 1097-1109. https://doi.org/10.1080/10942910903176360

Amipour, M., Shadizadeh, S. R., & Esfandyari, H. A. (2015). Experimental investigation of wettability alteration on residual oil saturation using nonionic surfactants: Capillary pressure measurement. *1*(4), 289-299. https://doi.org/10.1016/j.petlm.2015.11.003

Andersen, T. S. (2017). Cost Implications of Uncedrtainty in Carbon Dioxide Storage Resources-A Review. *Natural Resource Research, 26*(2), 137-159. https://doi.org/10.1007/s11053-016-9310-7

Andréa, L., Devaua, N., Pedenaud, P., & Azaroual, M. (2017). Silica Precipitation Kinetics: the Role of Solid Surface Complexation Mechanism Integrating the Magnesium Effects from 25 to 300 ℃. *Procedia Earth and Planetary Science, 17*, 217-220. https://doi.org/10.1016/j.proeps.2016.12.075

Arima, Y., & Iwata, H. (2007). Effect of Wettability and Surface Functional Groups on Protein Adsorption and Adhesion

Using Well-defined Mixed Self-Assembled Monolayers. *Biomaterials, 28*(20), 3074-3082. https://doi.org/10.1016/j.biomaterials.2007.03.013

Arsalan, N., Buiting, J. J., & Nguyen, Q. P. (2015). Surface energy and wetting behavior of reservoir rocks. *Colloids and Surfaces A: Physicochemical and Engineering Aspects, 467*, 107-112. https://doi.org/10.1016/j.colsurfa.2014.11.024

Asay, D. B., & Kim, S. H. (2005). Evolution of the Adsorbed Water Layer Structure on Silicon Oxide at Room Temperature. *Journal of Physical Chemistry B, 109*(35), 16760-16763. https://doi.org/10.1021/jp053042o

Atkinson, R. J., Posner, A. M., & Quirk, J. P. (1967). Adsorption of Potential-Determining Ions at the Ferric Oxide-Aqueous Electrolyte Interface. *Journal of Physical Chemistry, 71*(3), 550–558. https://doi.org/10.1021/j100862a014

Bachu, S., & Adams, J. (2003). Sequestration of CO2 in geological media in response to climate change: capacity of deep saline aquifers to sequester CO2 in solution. *Energy Conversion and Management, 44*(20), 3151-3175. https://doi.org/10.1016/S0196-8904(03)00101-8

Bain, C. D., & Whitesides, G. M. (1989). A Study by Contact Angle of the Acid-Base Behavior of Monolayers Containing -Mercaptocarboxylic Acids Adsorbed on Gold: An Example of Reactive Spreading. *Langmuir, 5*, Langmuir 1989, 5, 1370-1378. https://doi.org/10.1021/la00090a019

Barranco, Jr, F., Dawson, H., Christener, J. M., & Honeyman, B. D. (1997). Environ. Sci. Technol. *31*(3), 676-681. https://doi.org/10.1021/es960217m

Bellon-Fontaine, M. (1996). Microbial Adhesion to Solvents: a Novel method to Determine the Electron-Donor/electron-Acceptor or Lewis Acid-Base Properties of Microbial Cells. *Colloids and Surfaces B: Biointerfaces, 7*(1-2), 47-53. https://doi.org/10.1016/0927-7765(96)01272-6

Benjamin, M. L., Skylaris, C. K., & Green, N. G. (2015). Acid-base dissociation mechanisms and energetics at the silica–water. *Journal of Colloid and Interface Science, 451*, 231-244. https://doi.org/10.1016/j.jcis.2015.01.094

Berg, J. C. (2009). *An Introduction to Interfaces & Colloids: The Bridge to Nanoscience Paperback* . World Scientific Publishing. https://doi.org/10.1142/7579

Bickmore, B. R., Wheeler, J. C., Bates, B., Nagy, K. L., & Eggett, D. L. (2008) Reaction pathways for Quartz Dissolution Determined by Statistical and Graphical Analysis of Macroscopic Experimental Data. Geochim. Cosmochim. *Acta, 72*, 4521-4536. https://doi.org/10.1016/j.gca.2008.07.002

Bradely, J. M. (2005). Determining the Dispersive and Polar Contributions to the Surface Tension of Water-based Printing Ink as a Function ofSurfaxctant Surface Excess. *Journal of D:Applied Phys., 38*, 2045-2050. https://doi.org/10.1088/0022-3727/38/12/028

Brady, P. V., & Walther, J. V. (1989). Controls on silicate dissolution rates in neutral and basic pH solutions at 25℃. *Geochimica et Cosmochimica Acta, 53*(11), 2823-2830. https://doi.org/10.1016/0016-7037(89)90160-9

Buckingham, A. D., Fowler, P. W., & Hutson, J. M. (1988). Theoretical Studies of van der Waals Molecules and Intermolecular Forces. *Chem. Rev., 88*(6), 963-988. https://doi.org/10.1021/cr00088a008

Caroline-Michaliski, & Saramago, B. J. (2000). Static and Dynamic Wetting Behavior of triglycerine on Solid Surfaces. *Iournal of Colloid and Interfaces, 227*(2), 380-389. https://doi.org/10.1006/jcis.2000.6869

Carré, A., Lacarrière, V., & Birch, W. (2003). Molecular interactions between DNA and an aminated glass substrate. *Journal of colloid and interface science, 260*(1), 49-55. https://doi.org/10.1016/S0021-9797(02)00147-9

Chapelle, F. H., & Knobel, L. L. (1983). Aqueous Geochemistry and the Exchangeable Cation Composition of Glauconite in the Aquia Aquifer, Maryland. *Groundwater, 21*(3), 343-352. https://doi.org/10.1111/j.1745-6584.1983.tb00734.x

Chatelier, R. C., Drummond, C. J., Chan, D. Y., Vasic, Z. R., Gengenbach, T. R., & Griesser, H. J. (1995). Theory of Contact Angles and the Free Energy of Formation of Ionizable Surfaces: Application to Heptylamine Radio-Frequency Plasma-Deposited Films. *Langmuir, 11*(10), 4122-4128. https://doi.org/10.1021/la00010a078

Chattoraj, D. K., & Birdi, K. S. (1984). *Adsorption and the Gibbs Surface Excess.* New York: Plenum Press. https://doi.org/10.1007/978-1-4615-8333-2

Chau, L. K., & Porter, M. D. (1991). Surface isoelectric point of evaporated silver films: Determination by contact angle titration. *J. Colloid Interface Sci., 145*(1), 283-286. https://doi.org/10.1016/0021-9797(91)90121-N

Chen, C., Dong, B., Zhang, N., Li, W., & Song, Y. (2016). Pressure and Temperature Dependence of Contact Angles for

CO2/Water/Silica Systems Predicted by Molecular Dynamics Simulations. *Energy Fuels, 30*(6), 5027-5034. https://doi.org/10.1021/acs.energyfuels.6b00171

Chiu, V. C., Mouring, D., Watson, B. D., & Haynes, D. H. (1980). Measurement of Surface Potential and Surface Charge Densities of Sarcoplasmic Reticulum Membranes. *The Journal of Membrane Biology, 56*(2), 121-132. https://doi.org/10.1007/BF01875963

Dans, B. R., Moat, M. S., & Wang, S. (Eds.). (2018). Extraction 2018. *Procedings of the First Global Conference on Extractive Metallurgy.* Springer.

Deer, W. A., Howie, R. A., & Zussman, J. (1962). *Introduction to the Rock Forming Minerals.* Prentice Hall.

Dove, P. M. (1994). The Dissolution Kinetics of Quartz in Sodium Chloride Solutions at 25 °to 300 ℃. *Am. J. Sci., 294*, 665-712. https://doi.org/10.2475/ajs.294.6.665

Dreher, T., Lemarchand, C., Soulard, L., Bourasseau, E., Malfreyt, P., & Pineau. (2018). Calculation of a solid/liquid surface tension: A methodological study. *The Journal of Chemical Physics, 148*(3), 034702-9. https://doi.org/10.1063/1.5008473

Duana, Z., & Sun, R. (2003). An Improved Model Calculating CO2 Solubility in Pure Water and Aqueous NaCl solutions from 273 to 533 K and from 0 to 2000 bar. *Chemical Geology, 193*, 257-271. https://doi.org/10.1016/S0009-2541(02)00263-2

Espinoza, D. N., & Santamarina, J. C. (2010). Water-CO2-Mineral Systems: Interfacial Tension, Contact Angle and Diffusion—Implications to CO2 Geological Storage. *Water Resources Research, 46*, 1-10. https://doi.org/10.1029/2009WR008634

Feng, B., Lu, Y. P., Feng, Q. M., Ding, P., & Luo, N. (2013). Mechanisms of Curface Charge Development of Serpentine Mineral. *Trans. Nonferrous Met. Soc. China, 23*, 1123-1128. https://doi.org/10.1016/S1003-6326(13)62574-1

Fernandez-Toledano, J. C., Blake, T. D., & Coninck, J. D. (2017). Young's Equation for a Two-Liquid System on the Nanometer Scale. *Langmuir, 33*(11), 2929-2938. https://doi.org/10.1021/acs.langmuir.7b00267

Gao, L., & McCarthy, T. J. (2006). Contact Andgle Hysteresis Explained. *Langmuir, 22*(14), 6234-6237. https://doi.org/10.1021/la060254j

Gilfillan, S. M., Lollar, B. S., Holland, G., Blagburn, D., Stevens, S., Schoell, M., ... & Ballentine, C. J. (2009). Solubility Trapping in Formation Water as dominant CO2 Sink in Natural Gas Fields. *Nature, 458*, 614-618. https://doi.org/10.1038/nature07852

Glover, P. W., Meredith, P. G., & Sammonds, P. R. (1994, November 10). Ionic surface electrical conductivity in sandstone. *JOURNAL OF GEOPHYSICAL RESEARCH,AGES 21,635-21,650, NOVEMBER 10, 1994, 99*, (NO. Bll, P), 21,635-21,650.

Guo, S., Zhu, X., Li, M., Shi, Liya, Ong, J. L., ... & Neoh, K. G. (2016). Parallel Control over Surface Charge and Wettability Using Polyelectrolyte Architecture: Effect on Protein Adsorption and Cell Adhesion. *ACS Appl. Mater. Interfaces, 8*(44), 30552-30563. https://doi.org/10.1021/acsami.6b09481

Heller, W., Cheng, M. H., & Greene, B. (1966). Surface tension measurements by means of the "microcone tensiometer". *J. Colloid Interf Sci., 22*, 179-194. https://doi.org/10.1016/0021-9797(66)90082-8

Hille, B., Woodhull, A. M., & Shapiro, B. I. (1975). Negative surface charge near sodium channels of nerve: divalent ions, monovalent ions, and pH. *Phil. Trans. R. Soc. Lond., 301*(B 270), 301-318. https://doi.org/10.1098/rstb.1975.0011

Hogt, A. H., Gregonis, D. E., Andrade, J. D., Kim, S. W., Dankert, J., & Feijen, J. (. (1985). *Wettability and ζ potentials of a Series of Methacrylate Polymers and Copolymers. Journal of Colloid and Interface Science, 106*(2), 289-298. https://doi.org/10.1016/S0021-9797(85)80002-3

Holloway, S. (2001). Storage of Fossil Fuel-Derived Carbon Dioxide Beneath the Surface of the Earth. *Annual Review of Energy and the Environment, 26*, 145-166. https://doi.org/10.1146/annurev.energy.26.1.145

Holmes, C. F. (1973). On the Relation between Surface Tension and Dielectric Constant. *Journal of the American Chemical Society, 95*(4), 1014-1016. https://doi.org/10.1021/ja00785a004

Horiuchi, H., Nikolov, D., & Wasan, D. (2012). Calculation of the surface Potential and Surface Charge Density by Measurement of the Three-Phase Contact Angle. *Journal of Colloid and Interfac.* https://doi.org/10.1016/j.jcis.2012.06.078

Huang, W. T. (1962). *Petrology.* McGraw-Hill Book Company.

Jafari, M., & Jung, J. (2018). Variations of Contact Angles in Brine/CO2/Mica System Considering Short Term Geological Sequestration Conditions. *Geofluids*, 1-15. https://doi.org/10.1155/2018/3501459

Jiang, J., Guo, Q., Wang, B., Xu, L. Z., Deng, C., Yao, X., ... & Wang, J. (2016). Research on Variation of Static Contact Angle in Incomplete Wetting System and Modeling Method. *Colloids and Surfaces A: Physicochemical and Engineering Aspects, 504*, 400-406. https://doi.org/10.1016/j.colsurfa.2016.05.051

Joud, J., Houmard, M., Berthomé, G., & Berthomé, G. (2013). Surface Charges of Oxides and Wettability: Application to TiO2–SiO2 Composite Films. *Applied Surface Science, 287*(15), 37-45. https://doi.org/10.1016/j.apsusc.2013.09.054

Jung, J. W., & Wan, J. (2012). Supercritical CO2 and Ionic Strength Effects on Wettability of Silica Surfaces: Equilibrium Contact Angle Measurements. *Energy Fuels, 26*, 6053-6059. https://doi.org/10.1021/ef300913t

Kallay, N., Preočanin, T., Kovačević, D., Lützenkirchen, J., & Chibowskic, E. (2010). Electrostatic Potentials at Solid/Liquid Interfaces. *Croat. Chem. Acta, 83* (3), 357-370.

Kan, K. H. (2002). How Electrostatic Fields Change Contact Angle in Electrowetting,. *Langmuir, 18*, 10318-10322. https://doi.org/10.1021/la0263615

Kaveh, N. S., Rudolph, E. S., Hemert†, P. V., Rossen, W. R., & Wolf, K. H. (2014). Wettability Evaluation of a CO2/Water/Bentheimer Sandstone System: Contact Angle, Dissolution, and Bubble Size. *Energy Fuels, 28*(6), 4002-4020. https://doi.org/10.1021/ef500034j

Kim, Y., Jiamin, W., Kneafsey, T. J., & Tokunaga, T. K. (2012). Dewetting of Silica Surfaces upon Reactions with Supercritical CO2 and Brine: Pore-Scale Studies in Micromodels. *Environ. Sci. Technol., 46*(7), 4228–4235. https://doi.org/10.1021/es204096w

Knox, K. (1985). Le Châtelier's Principle. *J. Chem. Educ., 62*(10), 863. https://doi.org/10.1021/ed062p863

Kosmulski, M. (2002). The pH-Dependent Surface Charging and Points of Zero Charge V. Update. *Journal of Colloid and Interface Science, 253*, 77-87. https://doi.org/10.1006/jcis.2002.8490

Kosmulski, M. (2009). pH-Depended Surface Charging and Points of Zero Charge. IV.Update and New Approach. *Journal of Colloids and Interface Science, 337*, 439-448. https://doi.org/10.1016/j.jcis.2009.04.072

Kosmulski, M. (2011). The pH-dependent surface charging and points of zero charge: V. Update. *Journal of Colloid and Interface Science, 353*(1), 1-15. https://doi.org/10.1016/j.jcis.2010.08.023

Kozbial, A., Trouba, C., Liu, H., & Li, L. (2017). Characterization of the Intrinsic Water Wettability of Graphite Using Contact Angle Measurements: Effect of Defects on Static and Dynamic Contact Angles. *Langmuir, 33*(4), 959-967. https://doi.org/10.1021/acs.langmuir.6b04193

Light, T. S., & Licht, S. L. (1987). Conductivity and Resistivity of Water from the Melting to Critical Points. *Analytical Chemistry, 59*(19), 1987-2329. https://doi.org/10.1021/ac00146a003

Liu, J., Wani, O. B., Alhassan, S. M., & Pantelides, S. T. (2018). Wettability Alteration and Enhanced Oil Recovery Induced by Proximal Adsorption of Sodium, Chloride, Calcium and ions on Calcite. *Phys. Rev. Applied, 10*, 034064-034075. https://doi.org/10.1103/PhysRevApplied.10.034064

Long J., Hyder M. N., Huang R. Y., & Chen, P. (2005). Thermodynamic modeling of contact angles on rough, heterogeneous surfaces, *Adv Colloid Interface Sci., 118*(1-3), 173-190. https://doi.org/10.1016/j.cis.2005.07.004

Lowenstern, J. B. (2001). Carbon Dioxide in Magmas and Implications for Hydrothermal Systems. https://doi.org/10.1007/s001260100185

Lutzenkirchen, J. (1998). Comparison of 1-pk and 2-pk Version of Surface Complexation Theory bt the Goodness of Fit in Describing Surface Charge Data of Hydroxides. *Environmental Science and Technology, 32*(20), 3149-3154. https://doi.org/10.1021/es980125s

Lyklema, J. (1984). Points of zero charge in the presence of specific adsorption. *J. Colloid Interface Sci., 99*(1), 109-117. https://doi.org/10.1016/0021-9797(84)90090-0

Makkonen, L. (2016). Young's equation revisited. *J Phys Condens Matter, 28*(13), 1-4. https://doi.org/10.1088/0953-8984/28/13/135001

Maryott, A. A., & Smith, R. S. (1951). *Table of Dielectric Constants of Pure Liquids.* Washington , USA: National Bureau of Standards. https://doi.org/10.6028/NBS.CIRC.514

McCafferty, E., & Wightman, J. (1997). Determination of the Surface Isoelectric Point of Oxide Films on Metals by Contact Angle Titration. *Journal of Colloid and Interface Science, 194*(2), 344-355. https://doi.org/10.1006/jcis.1997.5138

Michael, K., & Aiken, T. (2010). Geological Storage of Carbon Dioxide in Saline Aquifers-A Review of the Experience from Existing Storage Operations. *International Journal og Greenhouse Gas Control, 4*(4), 659-667. https://doi.org/10.1016/j.ijggc.2009.12.011

Mohammadian, E., Hamidi, H., Asadullah, M., Azdarpour, A., Motamedi, S., & Junin, R. (2015). Measurement of CO2 Solubility in NaCl Brine Solutions at Different Temperatures and Pressures Using the Potentiometric Titration Method. *J. Chem. Eng. Data, 60* , 2042-2049. https://doi.org/10.1021/je501172d

Mohr, P. J., & Taylor, B. N. (1998). *Fundamental Physical Constants.* Retrieved from http://web.mit.edu/birge/Public/formulas/phys-const.pdf

Millero, F. J., Pierrot, D., Lee, K., Wanninkhol, R., Feely, R., Sabine, L. C., ... & Takahashi. (2002). Dissociation Constants for Carbonic Acid Determined from Field Measurements. *Deep Sea Research, 1*(49), 1705-1723. https://doi.org/10.1016/S0967-0637(02)00093-6

NIST. (2015, June). *The NIST Reference on Constants, Units, and Uncertainty. US National Institute of Standards and Technology.* Retrieved from Faraday Constant: http://www.wikiwand.com/en/Faraday_constant

Orumwense, F. O. (1998). Estimation of the wettability of coal from contact angles using coagulants and flocculants. *Fuel, 77*(9-8), 1107-1111. https://doi.org/10.1016/S0016-2361(97)00223-8

Oss, V. C. (1993). Acid-base Interfacial Interactions in Aqueous Media. *Colloids and Surfaces A: Physicochemical and Engineering Aspects, 78*(1), 1-49. https://doi.org/10.1016/0927-7757(93)80308-2

Orumwense, F. O. (2001). Wettability of coal – a comparative study. *Scandinavian Journal of Metallurgy, 30*, 204–211. https://doi.org/10.1034/j.1600-0692.2001.300402.x

Oss, C. J., Good, R. J., & Chaudhury, M. K. (1988). Additive and nonadditive surface tension components and the interpretation of contact angles. *Langmuir, 4*(4), 884-891. https://doi.org/10.1021/la00082a018

Oss, C. J. (2006). *Interfacial Forces in Aqueous Media-Second Edition.*

Park, J. H., Schwartz, Z., Olivares-Navarrete, R., Boyan, B. D., & Tannenbaum, R. (2011). Enhancement of Surface Wettability via the Modification of Microtextured Titanium Implant Surfaces with Polyelectrolytes. *Langmuir, 27*(10), 5976-5985. https://doi.org/10.1021/la2000415

Parks, G. A. (1984). Surface and Interfacial Free Energy of Quartz. *Journal of Geophysical Research, 89*(86), 3997-4008. https://doi.org/10.1029/JB089iB06p03997

Parks, G. A. (1984). Surface Energies of Quartz. *Journal OF Geophysical Research, 89*(B6), 3997-4008. https://doi.org/10.1029/JB089iB06p03997

Philipsea, A., Tuiniera, R., Kuipersa, B., Vrija, A., & Vis, M. (2017). On the Repulsive Interaction Between Strongly Overlapping Double Layers. *Colloid and Interface Science Communications, 21*, 10-14. https://doi.org/10.1016/j.colcom.2017.10.002

Plasecki, W., Rudzinski, W., & Charmas, R. (2001). 1-pk and 2-pk Models in the Theoretical Description of Simple Ion Adsorption at thge Oxide/Electrolyte Interface: a Copmparative Study of the Behavior of the Surface Charge, the Individual Isotherms of ions, and the Accompanying Electrokinetic Effect. *Joournal of Physics Chemistry B, 105*(40), 9755-9771. https://doi.org/10.1021/jp011299q

Portia, S., & Rochelle, C. (2005). Modelling Carbon Dioxide Solubility in Pure Water and NaCl-Type Waters from 0-to 300 Degrees Celsius and from1 to 300 Bar: Application to the UtsiraFormation at Sleipner. *Chemical Geology, 217*, 187-199. https://doi.org/10.1016/j.chemgeo.2004.12.007

Preoanin, T., & Kallay, N. (2006). Point of Zero Charge and Surface Charge Density of TiO2 in Aqueous Electrolyte Solution as Obtained by Potentiometric Mass Titration. *Croat. Chem. Acta, 79*(1), 95-106.

Puah, L. S., Sedev, R., Fornasiero, D., Ralston, J., & Blake, T. (2010). Influence of Surface Charge on Wetting Kinetics. *Langmuir, 26*(22), 17218-17224. https://doi.org/10.1021/la103351t

Rimstidt, J. D. (2015). Rate equations for sodiumcatalyzed quartz dissolution. *Geochim. Cosmochim Acta, 167*, 195-204. https://doi.org/10.1016/j.gca.2015.07.030

Ratajczak, T., & Drzymala, J. (2012). Excess interfacial energy change of solid/aqueous salt solution system with increasing salt concentration at a constant charge-determining ion activity based on

https://doi.org/10.2478/s11532-012-0118-y

Rosenbauer, R., & Koksalan, T. (2004). Experimental Multi-Phase H2O-CO2 Brine Interactions at Elevated Temperature and Pressure: Implications for CO2 sequestration in deep-saline aquifers. *Am. Chem. Soc., Div. Fuel Chem., 49*(1), 416-417.

Schneemilch, M., Welters, W. J., Hayes, R. A., & Ralston, J. (2000). Electrically Induced Changes in Dynamic Wettability. *Langmuir, 16*, 2924-2927. https://doi.org/10.1021/la990524g

Schön, J. H. (2015). *n Developments in Petroleum Science.* Elsevier.

Sedwick, P. N., & Goff, F. (1994). Carbon Dioxide and Helium in Hydrothermal Fluids from Loihl Seamount, Hawaii, USA: Temporal Variability and Implications for the Release of Mantle Volatiles. *Geochimichimica et Cosmochimica Acta, 58*(3), 1219-1227. https://doi.org/10.1016/0016-7037(94)90587-8

Solomon, T. (2001). The Definition and Unit of Ionic Strength. *J. Chem. Educ., 78*(12), 1691. https://doi.org/10.1021/ed078p1691

Sonnefeld, J. (2001). On the Influence of Background Electrolyte Concentration on the Position of the isoelectric Point and the Point of Zero Charge. *Colloids Surf. A, 190*(1-2), 179-183. https://doi.org/10.1016/S0927-7757(01)00677-X

Soong, Y., Goodman, A., McCarthy-Jones, R., & Baltrus, J. (2004). Experimental and Simulation Studies on Mineral Trapping of CO2 with Brine. *Energy Conversion and Management, 45*(11-12), 1845-1859. https://doi.org/10.1016/j.enconman.2003.09.029

Sposito, G. (1998). On points of zero charge. *Environmental science & technology, 32*(19), 2815-2819. https://doi.org/10.1021/es9802347

Stogryn, A. (1971). Equations for Calculating the Dielectric Constant of Saline Water. *IEEE Transactions, 19*, 733-736. https://doi.org/10.1109/TMTT.1971.1127617

Sverjensky, D. A. (2005). Prediction of Surface Chrage on Oxide sin Salt Solutions:Predictio for 1:1 (M L) Solutions. *Geochimica et Cosmochimica Acta, 69*(2), 225-257. https://doi.org/10.1016/j.gca.2004.05.040

Tamura, H., Mita, K., Tanaka, A., & Makoto, I. (2001). Mechanism of Hdroxyllation of Metal Oxides Surfaces. *Joournal 0f Colloid and Interface Science, 243*, 202-207. https://doi.org/10.1006/jcis.2001.7864

Trinh, T., Bedeaux, D., Simon, J., & Kjelstrup, S. (2015). Calculation of the chemical potential and the activity coefficient of two layers of CO2 adsorbed on a graphite surface. *Phys Chem Chem Phys., 17*(2), 1226-1233. https://doi.org/10.1039/C4CP03782K

Ward, C. A., & Wu, J. (2007). Effect of Adsorption on the Surface Tensions of Solid-Fluid Interfaces. *J. Phys. Chem. B, 111*, 3685-3694. https://doi.org/10.1021/jp067066m

Webb, K., Vladimir, H., & Tresco, P. A. (1998). Relative Importance of Surface Wettability and Charged Functional Groups on NIH 3T3 Fibroblast Attachment, Spreading, and Cytoskeletal Organization. *J Biomed Mater Res., 41*(3), https://doi.org/10.1002/(SICI)1097-4636(19980905)41:3<422::AID-JBM12>3.0.CO;2-K

Zhu, D., Pin, P., & Luo et al. (2007). Novel characterization of wetting properties and the calculation of liquid–solid interface tension (I)," Science Technology and Engineering. *Science Technology and Engineering, 7*(13), 3057-3062.

Zhuravlev, L. T. (1987). Concentration of hydroxyl groups on the surface of amorphous silicas. *Langmuir, 3*(3), 316-318. https://doi.org/10.1021/la00075a004

Appendices

Appendix 1: Parabolic variation of the cosine of the contact angle on the PTS-treated glass as a function of pH of aqueous solution (Carre *et al*., 2003)

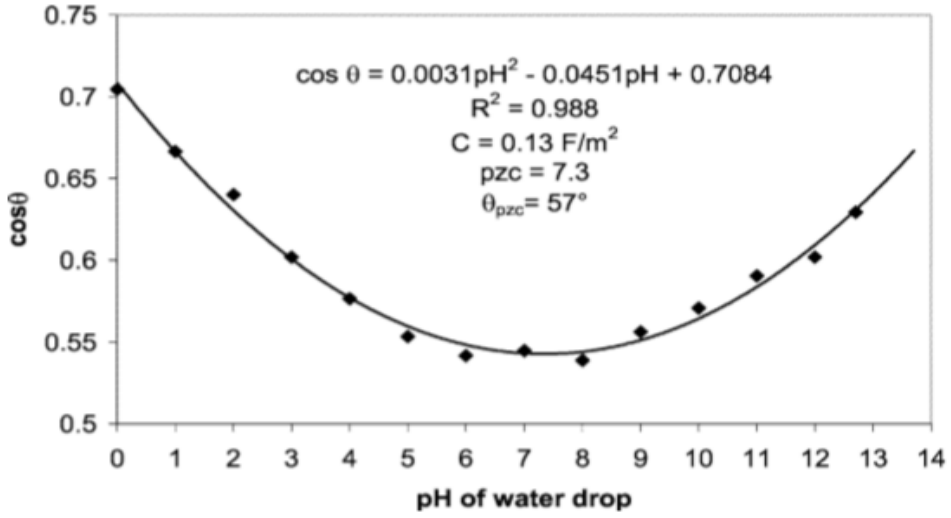

Appendix 2: Computed values of cosine of contact angle using our model (Eq. (50)) and that of Carre *et al*., (2003)

pH	Values using our model	Experimental Values	Difference	Fractional Error
1	0.700	0.666	0.033	0.050
1.5	0.677	0.648	0.030	0.046
2	0.657	0.631	0.026	0.042
2.5	0.638	0.615	0.023	0.038
3	0.622	0.601	0.021	0.034
3.5	0.607	0.589	0.018	0.031
4	0.594	0.578	0.016	0.028
4.5	0.582	0.568	0.014	0.025
5	0.573	0.560	0.013	0.022
5.5	0.565	0.554	0.011	0.020
6	0.560	0.549	0.010	0.019
6.5	0.556	0.546	0.010	0.018
7	0.554	0.545	0.009	0.017
7.5	0.554	0.545	0.009	0.017
8	0.556	0.546	0.010	0.018
8.5	0.559	0.549	0.010	0.018
9	0.565	0.554	0.011	0.020
9.5	0.572	0.560	0.012	0.022
10	0.581	0.567	0.014	0.024
10.5	0.592	0.577	0.015	0.027
11	0.605	0.587	0.017	0.030
11.5	0.619	0.600	0.020	0.033
12	0.636	0.614	0.022	0.037
12.5	0.654	0.629	0.025	0.040

Appendix 3: Contact angle on silica versus pressure as a function of salinity (Jung and Wan, 2012)

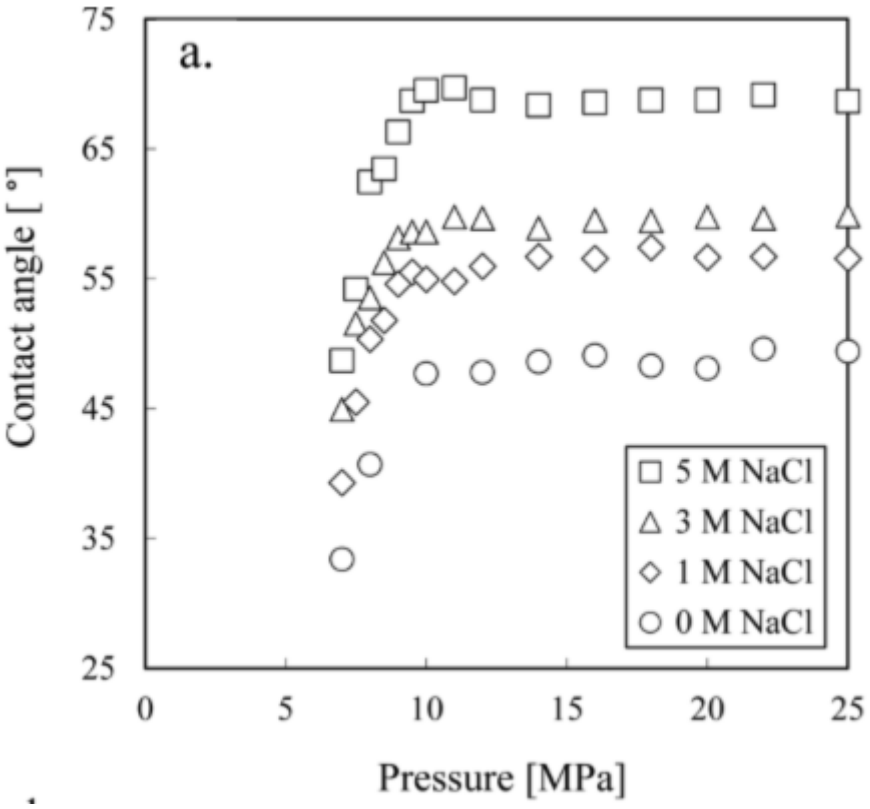

Appendix 4: Surface potential versus Ph as a function of aqueous solution salinity (Hille *et al*., 1975)

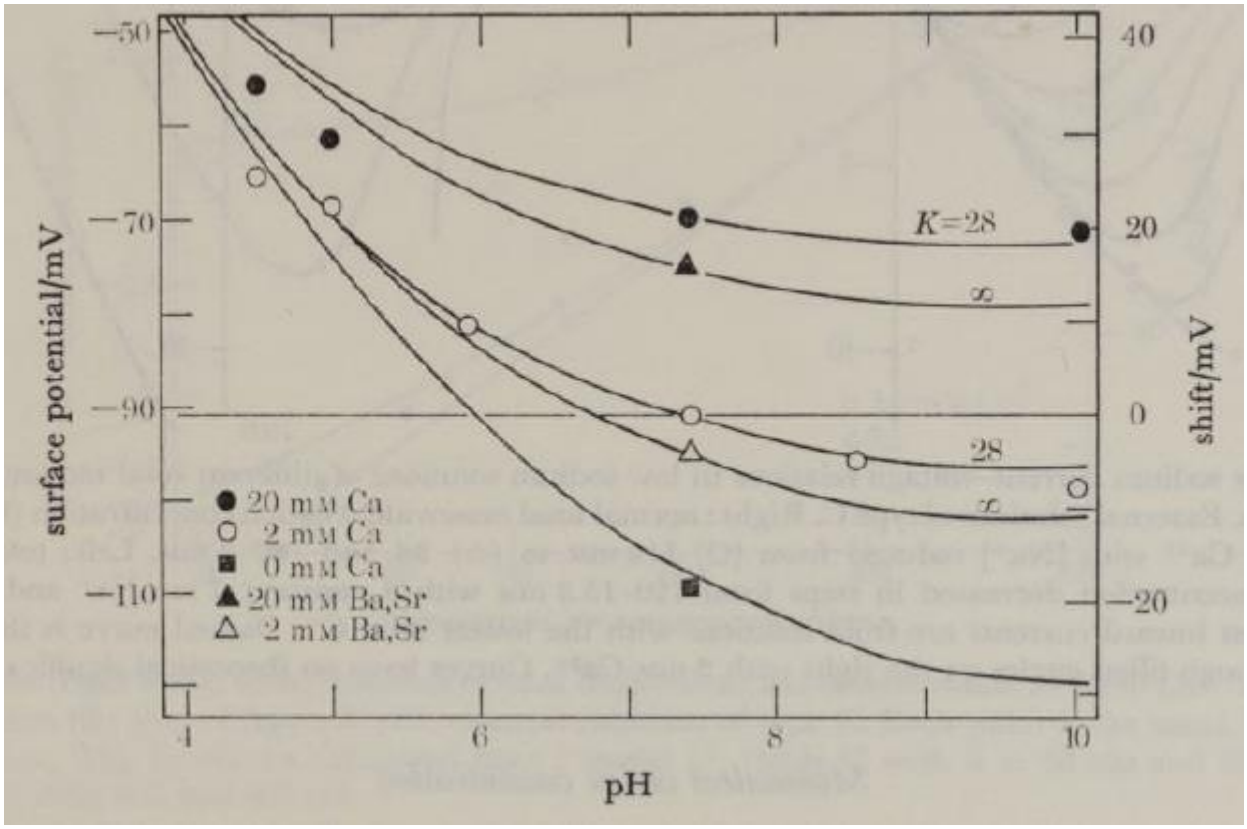

Appendix 5: Surface charge density versus pH as a function of salinity (Sverjensky, 2005)

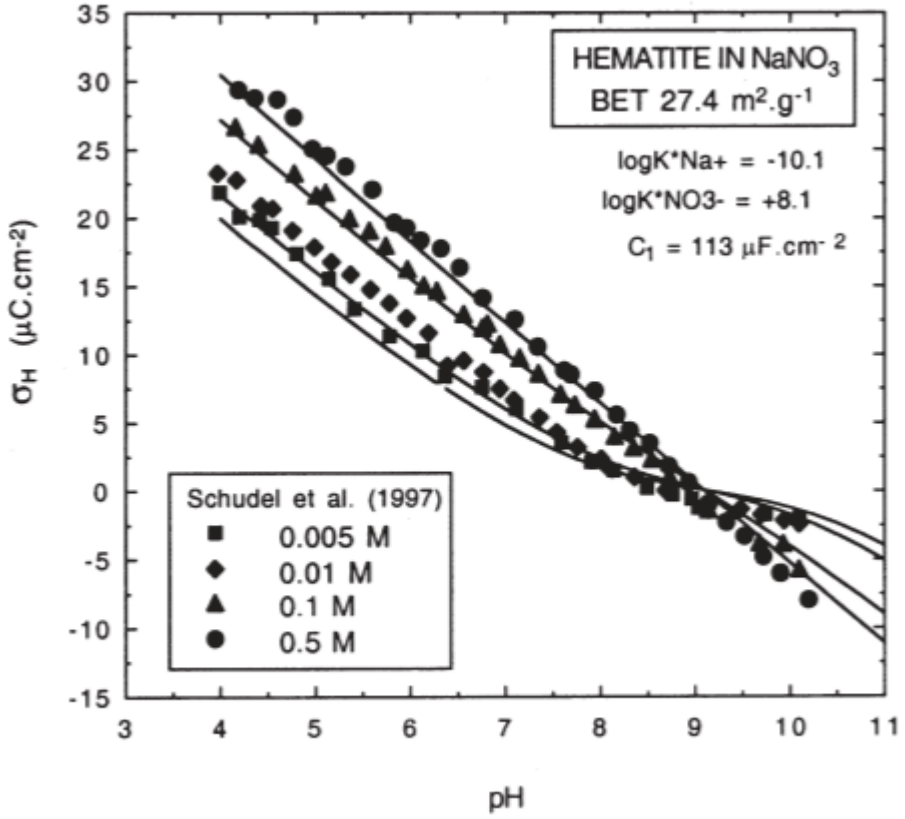

Appendix: 6: Final contact angle plots versus pressure for mica surface showing parabolic trends (Jafari & Jung, 2018)

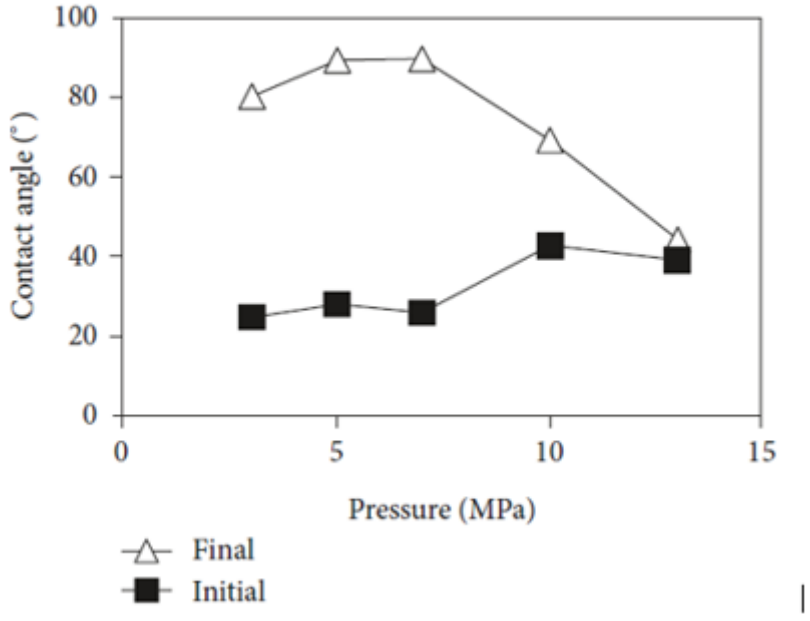

Appendix 7: Variation of the three-phase contact angle of aqueous solutions on a mica sheet with pH (Horiochi *et al.*, 2012)